

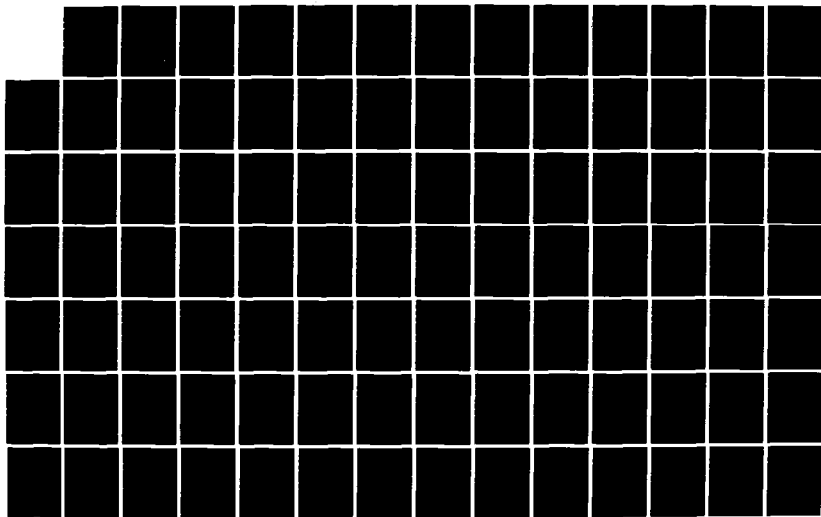
AD-A159 244

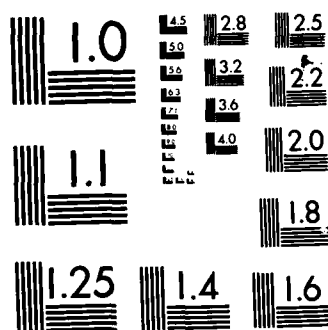
IDENTIFICATION OF NUCLEAR MATERIALS FROM REMOTE  
DETECTION OF CHARACTERIST (U) AIR FORCE INST OF TECH  
WRIGHT-PATTERSON AFB OH SCHOOL OF ENGI L W BRASURE  
MAR 85 AFIT/GNE/PH/85M-2 F/G 18/4

1/2

UNCLASSIFIED

NL





AD-A159 244



IDENTIFICATION OF NUCLEAR MATERIALS  
FROM REMOTE DETECTION OF  
CHARACTERISTIC GAMMA RAYS

THESIS

L. Wayne Brasure  
Captain, USAF

AFIT/GNE/PH/85M-2

This document has been approved  
for public release and sale; its  
distribution is unlimited.

DEPARTMENT OF THE AIR FORCE  
AIR UNIVERSITY

**AIR FORCE INSTITUTE OF TECHNOLOGY**

Wright-Patterson Air Force Base, Ohio

85 09 17 030

DTIC FILE COPY

DTIC

SEL

SEP 18 1985

A

AFIT/GNE/PH/85M-2

IDENTIFICATION OF NUCLEAR MATERIALS  
FROM REMOTE DETECTION OF  
CHARACTERISTIC GAMMA RAYS

THESIS

L. Wayne Brasure  
Captain, USAF

AFIT/GNE/PH/85M-2

Approved for public release; distribution unlimited

SEP 18 1985

A

AFIT/GNE/PH/85M-2

IDENTIFICATION OF NUCLEAR MATERIALS FROM REMOTE DETECTION OF  
CHARACTERISTIC GAMMA RAYS

THESIS

Presented to the Faculty of the School of Engineering  
of the Air Force Institute of Technology

Air University

In Partial Fulfillment of the  
Requirements for the Degree of  
Master of Science in Nuclear Physics

L. Wayne Brasure, B.S., M.S.S.M.  
Captain, USAF

March 1985

Accession For	
NTIS GRA&I	<input checked="checked" type="checkbox"/>
DTIC TAB	<input type="checkbox"/>
Unannounced	<input type="checkbox"/>
Justification	
By	
Distribution/	
Availability Codes	
Avail and	
Part	Spec

AT



Approved for public release; distribution unlimited

## Preface

The purpose of this thesis was to investigate a method of extending the range of identification of nuclear sources. The method was centered on Bayes' theorem, and the results were compared with the method of photopeak identification, which is perhaps the most common method used today. The Finite Element Method was used to transport the source spectra out to various ranges and Bayes' theorem, in conjunction with various statistical distributions, was used to analyze the results.

I would like to thank Dr. Larry McKee for sponsoring this thesis topic, and for his patience while I stumbled through some of the rough spots. I would also like to thank Dr. Donn Shankland for the countless hours spent helping me with statistical distributions, the Finite Element Method, and the Harris 800 operating system. Without him, none of this work would have been possible. In addition, I must express my gratitude to Mr. Seth Tuuri, for asking the fundamental questions that keep basic research alive.

Lastly and most importantly, I thank my wife and fellow classmate LeAnn, for sharing the frustrations and unreasonable hours along with me.

## Table of Contents

Preface . . . . .	ii
List of Figures . . . . .	v
List of Tables . . . . .	vi
Abstract . . . . .	viii
I. Introduction . . . . .	1
The Problem . . . . .	2
Approach . . . . .	3
Limitations . . . . .	4
Layout of Chapters . . . . .	5
II. Source Selection . . . . .	6
The Library Spectra . . . . .	6
III. Transport of Source Spectra . . . . .	14
Assumptions . . . . .	14
Overview of the Approach . . . . .	15
Source Transport . . . . .	25
IV. Identification and Analysis of Source Spectra . . . . .	40
Bayes Theorem . . . . .	40
V. Results and Discussion . . . . .	50
Bayes' Theorem with Poisson: No Background . . . . .	50
Bayes' Theorem with Multinomial: No Background . . . . .	61
Bayes' Theorem with Poisson: With Background . . . . .	64
The Unidentified Source . . . . .	66
Applying the Results . . . . .	72
VI. Summary and Recommendations . . . . .	74
Recommendations . . . . .	75
Appendix A: Photopeak Analysis Considerations . . . . .	77
Appendix B: 18 Gamma Group Cross Sections . . . . .	82
Appendix C: Simplifying the Three-Dimensional Transport Problem . . . . .	90

Appendix D:	The Analytical Solution (Simple Case) . . . . .	92
Appendix E:	Transport Code Listing . . . . .	95
Appendix F:	Generating Poisson and Multinomial Reference Values . . . . .	.114
Appendix G:	Generating Measured Source Spectra . . . . .	.119
Appendix H:	Analysis Code Listing . . . . .	.123



### List of Figures

Figure	Page
1. The Library Sources . . . . .	13
2. One-Dimensional Version of $F(1_1, 1_2)$ . . . . .	19
3. Finite Elements Solution Verification . . . . .	23
4. Reference Source A at 50, 100 & 200 Meters . . . . .	28
5. Reference Source A at 300, 400 & 500 Meters . . . . .	29
6. Reference Source B at 50, 100 & 200 Meters . . . . .	30
7. Reference Source B at 300, 400 & 500 Meters . . . . .	31
8. Reference Source C at 50, 100 & 200 Meters . . . . .	32
9. Reference Source C at 300, 400 & 500 Meters . . . . .	33
10. Posterior Distributions: Poisson . . . . .	60
11. Posterior Distributions: Multinomial . . . . .	63
12. Posterior Distributions: Poisson with Background . . . . .	68
13. The High Resolution Bin Structure . . . . .	80

### List of Tables

Table	Page
II-1	Energy Dependence of Detector Channels . . . . . 10
II-2	Relative Intensity Distribution of Library Sources (counts/photon) . . . . . 11
II-3	Relative Intensity Distribution of Library Sources (counts/KeV/photon) . . . . . 12
III-1	Relative Intensity Distribution of Reference Source A (50 - 200 meters) . . . . . 34
III-2	Relative Intensity Distribution of Reference Source A (300 - 500 meters) . . . . . 35
III-3	Relative Intensity Distribution of Reference Source B (50 - 200 meters) . . . . . 36
III-4	Relative Intensity Distribution of Reference Source B (300 - 500 meters) . . . . . 37
III-5	Relative Intensity Distribution of Reference Source C (50 - 200 meters) . . . . . 38
III-6	Relative Intensity Distribution of Reference Source C (300 - 500 meters) . . . . . 39
IV-1	Sample Prior Distribution . . . . . 44
V-1	Bayes' Posterior Distribution (Poisson with no background) . . . . . 52
V-2	Measured Source A (Poisson Distribution) 50 - 200 meters . . . . . 53
V-3	Measured Source A (Poisson Distribution) 300 - 500 meters . . . . . 54
V-4	Measured Source B (Poisson Distribution) 50 - 200 meters . . . . . 55
V-5	Measured Source B (Poisson Distribution) 300 - 500 meters . . . . . 56
V-6	Measured Source C (Poisson Distribution) 50 - 200 meters . . . . . 57
V-7	Measured Source C (Poisson Distribution) 300 - 500 meters . . . . . 58

V-8	Bayes' Posterior Distribution (Multinomial with No Background) . . . . .	62
V-9	Relative Intensity and Count Levels of Background . . . . .	65
V-10	Bayes' Posterior Distribution (Poisson with Background) . . . . .	67
V-11	Measured Source A (Poisson Distribution with Background) . . . . .	69
V-12	Measured Source B (Poisson Distribution with Background) . . . . .	70
V-13	Measured Source C (Poisson Distribution with Background) . . . . .	71
A-1	Photopeak Degradation . . . . .	81

## Abstract

This research effort studies the application of Bayes' decision theorem to extending the range of remote identification of nuclear materials. The Finite Element Method was used to develop a radiation transport code which was used to reconstruct a group of three sample sources at distances of 50, 100, 200, 300, 400 and 500 meters. Both the Poisson and multinomial distributions were then used to simulate measured sources in a low count environment at these six ranges. Bayes' theorem was applied to the resulting measured sources to test for positive identification.

The results show that a low resolution detector can increase the range of remote detection an average of 100 meters when compared with the method of photopeak identification. Bayes' theorem is unable, however, to identify sources not contained in the library of known sources.

*20-10-1984*

# IDENTIFICATION OF NUCLEAR MATERIALS FROM REMOTE DETECTION OF CHARACTERISTIC GAMMA RAYS

## I. Introduction

### Background

This thesis addresses the problem of identifying specific radioactive sources by examining their characteristic gamma ray spectra. The primary effort will be to develop a technique of extending the range of reliable detection of nuclear materials.

Normally, the analysis of characteristic gamma ray spectra involves matching the photopeaks of the given spectrum with those present in the spectra of known isotopes for the purpose of identifying the constituents of the source. Such identification of nuclear material is of interest in order to learn the nature of given sources, that is, to identify the 'ingredients' of a nuclear source. However, current methods which use photopeak analysis for identification purposes are of limited value once downscattering of the peak energies has occurred.

In order to be of practical benefit, the identification of nuclear materials must consider the non-ideal case of remote detection. In other words, the given gamma ray source spectrum must be examined at a distance and therefore, will have been transported through the atmosphere for a predetermined distance. Transporting such a spectrum through

air introduces a number of complications due to the interaction of photons with molecules and atoms in the earth's atmosphere.

By interacting with the particles of the air, photon energy is degraded by three main processes: the photoelectric effect, compton scattering, and pair production. The importance of each process depends on the initial energy of the photon. It is important here to realize that the compton scattering process is responsible for degrading the ideal (untransported) gamma spectrum by 'smearing' the energy of the photons over a wide range of values. Therefore, Compton scattering is the primary mechanism for the degradation of gamma photopeaks in this problem.

### The Problem

This thesis will study the ability to discriminate between different gamma ray source spectra by using Bayes' theorem. Bayes' theorem will be employed as a decision aid to assess the probability of having a certain source, given the transported spectrum. By plotting the probabilities as a function of distance from the source, we can determine the reliability of Bayes' theorem as a correlation technique for extending spectral identification beyond the current limitations of photopeak analysis.

Simply stated, this thesis will test the assumption that Bayes' theorem will work at distances from the source where

less than ideal circumstances include measuring a given source once at extreme range with a small number of counts collected.

#### Methodology: the Finite Elements Method

The method used to approximate the solution to the diffusion equation is the Finite Elements Method. It was chosen because of its accuracy in comparison to other methods such as the Method of Integration and it is at the same time less complicated to program than more advanced methods (8). In general, the diffusion equation is expressed as

$$-\nabla \cdot (D \nabla F) + \Sigma^a F = S \quad (1)$$

where the variable  $D$  is the diffusion coefficient,  $\Sigma^a$  is the macroscopic absorption cross section,  $S$  is the source function, and  $F$  is the fluence. Also, it is important to note that

$$D = \frac{1}{3\Sigma^{tr}} \quad (2)$$

where,  $\Sigma^{tr}$  is the macroscopic transport cross section. The Finite Elements Method assigns a penalty function given by

$$P(F) = \frac{1}{2} \int dV (D \nabla F \cdot \nabla F + \Sigma^a F^2 - 2FS) \quad (3)$$

### Overview of the Approach

The radiation transport problem will be solved by implementing a numerical solution to the diffusion equation. The diffusion equation will then be used to solve for the scattered fluence contribution of each energy group in each source. This scattered, or diffuse solution (including downscattering and inscattering contributions) will be added to the uncollided fluence (virgin fluence) solution of each energy group, resulting in a value of total fluence for each energy group.

By solving the diffusion equation for each library source at a number of different ranges, the reference sources are arrived at, which will be discussed later in this chapter. As the distance increases from the source, the uncollided fluence drops off exponentially (see appendix A), and at some point, there is an extremely small contribution to the solution due to the uncollided fluence, but still a sizable contribution from the diffuse (collided) fluence. In other words, the further away from the source the measurement is taken, the larger is the percentage of diffuse fluence. At some very large distance then, all the photons detected will have been scattered at least once, and therefore no more uncollided fluence is present. The concept of using Bayes' theorem as an analysis tool is based on using the diffuse solution in addition to the uncollided solution to identify sources measured under less than ideal circumstances. These



### III. Transport of Source Spectra

In the last chapter, a number of source spectra were introduced, based on high resolution data obtained at the surface of each source. Recall that the spectral distribution for each source was given in counts per gamma photon per unit energy, or alternately, in counts per photon per channel (each energy group representing a channel). In this chapter, the methodology will be developed to transport each of these library spectra to any given distance away from the original source. The results of the radiation transport of each of the three library sources will be presented at the end of this chapter.

#### Assumptions

In order to simplify the radiation transport problem into a manageable one, the following assumptions are made:

- (1) The source photons are transported through homogeneous air.
- (2) The source and the detector are located at sea level.
- (3) An ideal detector is assumed, so that all photons reaching the detector are counted.
- (4) The fluence of photons is radially symmetric (no angular dependence).

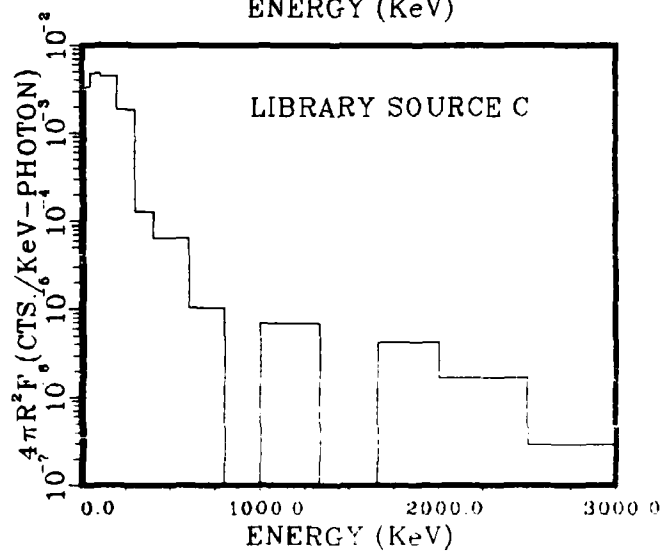
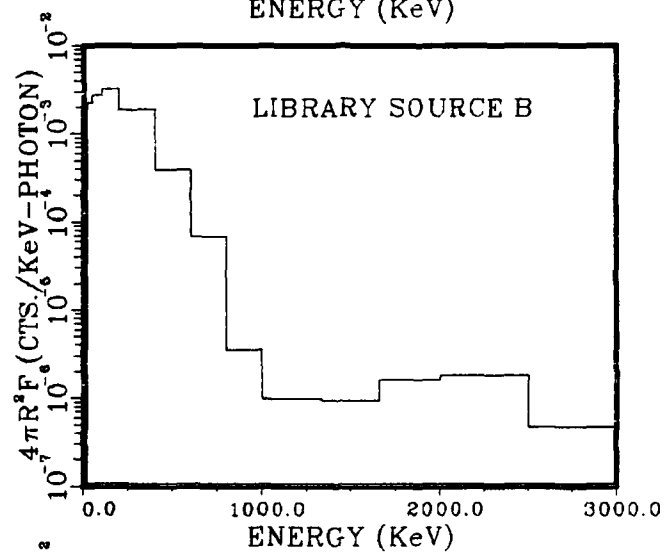
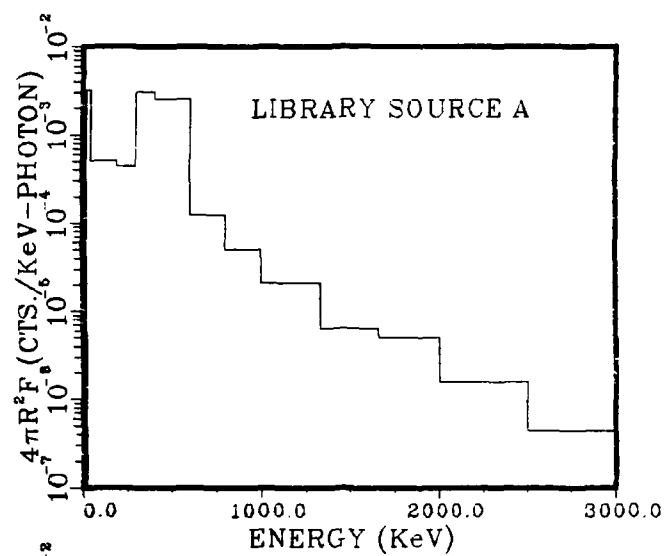


Figure 1. The Library Sources

TABLE II-3

## Relative Intensity Distribution of Library Sources

(counts / KeV / photon)

<u>Group Number</u>	<u>Source A</u>	<u>Source B</u>	<u>Source C</u>
1	0.0	0.0	0.0
2	0.0	0.0	0.0
3	0.0	0.0	0.0
4	0.0	0.0	0.0
5	0.0	0.0	0.0
6	4.39E-7	4.74E-7	2.93E-7
7	1.58E-6	1.81E-6	1.67E-6
8	4.99E-6	1.61E-6	4.21E-6
9	6.39E-6	9.36E-7	0.0
10	2.12E-5	9.81E-7	6.88E-6
11	5.00E-5	3.53E-6	0.0
12	1.23E-4	6.76E-5	1.04E-5
13	2.58E-3	3.95E-4	6.38E-5
14	3.06E-3	1.91E-3	1.28E-4
15	4.46E-4	1.87E-3	1.83E-3
16	5.09E-4	3.24E-3	4.43E-3
17	5.16E-4	2.69E-3	4.82E-3
18	3.27E-3	2.24E-3	3.34E-3

TABLE II-2  
Relative Intensity Distribution of Library Sources  
(counts / photon)

<u>Group Number</u>	<u>Source A</u>	<u>Source B</u>	<u>Source C</u>
1	0.0	0.0	0.0
2	0.0	0.0	0.0
3	0.0	0.0	0.0
4	0.0	0.0	0.0
5	0.0	0.0	0.0
6	2.20E-4	2.37E-4	1.47E-4
7	7.92E-4	9.06E-4	8.35E-4
8	1.70E-3	5.46E-4	1.43E-3
9	2.11E-3	3.09E-4	0.0
10	6.99E-3	3.24E-4	2.27E-3
11	1.00E-2	7.07E-4	0.0
12	2.47E-2	1.35E-2	2.08E-3
13	5.16E-1	7.90E-2	1.28E-2
14	3.06E-1	1.91E-1	1.28E-2
15	4.46E-2	1.87E-1	1.83E-1
16	5.09E-2	3.24E-1	4.43E-1
17	2.58E-2	1.34E-1	2.41E-1
18	9.80E-2	6.73E-2	1.00E-1

TABLE II-1  
Energy Dependence of Detector Channels

<u>Group Number</u>	<u>Energy (KeV)</u>
1	8000 - 10000
2	6500 - 8000
3	5000 - 6500
4	4000 - 5000
5	3000 - 4000
6	2500 - 3000
7	2000 - 2500
8	1660 - 2000
9	1330 - 1660
10	1000 - 1330
11	800 - 1000
12	600 - 800
13	400 - 600
14	300 - 400
15	200 - 300
16	100 - 200
17	50 - 100
18	20 - 50

"detector" is provided in table II-1. The 18 gamma-group cross section data file is attached in appendix B.

The second step involved totalling the counts contained in each of the newly defined eighteen channels for each source. In addition, the background data was subdivided into the eighteen channel structure.

Finally, the background was subtracted from each of the sources, and the total number of counts was determined for each. The relative intensity of each source was determined by dividing the number of counts in each channel by the total number of counts for that particular source. These relative intensities are provided in Table II-2. The final library spectra are pictured in figure 1, and a listing of the relative intensities in counts per KeV per photon are given in table II-3.

As can be seen in figure 1, all three sources have identifying features that makes each one unique. Sources B and C show the most similarities with respect to each other, and can be used as a benchmark during the analysis section, as mentioned earlier. As the transport distance increases, downscattering of gamma photons should make sources B and C 'converge' to a common spectrum, whereas source A should maintain its unique identity for larger ranges.

In the next chapter, the results of the radiation transport code development will be used to generate the measured and reference sources, based on the library sources presented in this chapter.

photopeak identification requires that a photopeak be at least three standard deviations above the background level for positive identification (three sigma being 99.7 percent probability of certainty). Please reference appendix A for more details on this subject.

Some notable photopeaks observed in the high resolution spectra include the 767 KeV and 1001 KeV lines from  $^{238}\text{U}$  and the 375 KeV and 414 KeV lines of  $^{239}\text{Pu}$ . Numerous other photopeaks from other radioisotopes contribute to the overall relative intensities in each channel.

The second criterion listed above will test how Bayes Decision Theory can discriminate between two similar nuclear sources, in contrast to two sources which have dissimilar spectral features. In addition, a fourth source will be introduced, which will be different from all of the library spectra, in order to examine the effects of an "unknown" source on the analysis.

#### Creation of the Low Resolution Sources.

Having selected the three high resolution spectra (in line with the above criteria), the task remains to translate these into the three low resolution library spectra for use in this problem. This was accomplished in three basic steps.

First, the high resolution spectral data was divided into an eighteen energy group structure, which was used in this problem. The eighteen group structure was chosen because the gamma photon cross section data was readily available (14). The energy structure of this low resolution

spectra were obtained using a high resolution Germanium detector, and exhibited detailed line structure and continuum levels.

All of the above mentioned measurements were made within one meter of each source, and each source was enclosed within a container. Therefore, the spectra represent the characteristic source spectra taken at the surface of the source, and some downscattering of the photons has already occurred. The library sources derived from this data therefore represent each spectrum taken at the surface of each nuclear source.

#### Generation of Library Spectra.

##### Selection of the High Resolution Sources.

The three library sources were composed using the data discussed above. These library spectra were taken directly from three of the measured (high resolution) gamma spectra, based on the following criteria:

- (1) Each source should contain discernible photopeaks (at least three standard deviations above the background).
- (2) Two of the sources should have some similar spectral features and relative intensities, and the third should not strongly resemble the others.

Using the first criterion will allow for a contrast with the method of photopeak identification, which classifies nuclear materials by identifying specific (characteristic) lines in the spectrum. As mentioned above, the method of



## II. Source Selection

The first order of business in this problem is to identify several source spectra that will represent the gamma ray signature of different nuclear materials. These source spectra, or "library spectra," will then be used to test the feasibility of Bayes Theorem as a remote identification tool.

### The Library Spectra

#### Method of Selection.

There are two possible approaches to the source selection process. In the first approach, the library spectra are chosen to represent the gamma spectra of specific radioisotopes, that is, each source is composed of a simple combination of radioisotopes, with the intensity levels determined arbitrarily. Using a second approach, the library spectra represent actual nuclear materials. By using the second method, the intensity levels of the library spectra are more realistic, having been taken from actual measurements of different nuclear materials.

The second method of source selection was used in this research project, in order to more realistically assess the utility of Bayes Theorem as a method of remote source identification.

#### Spectral Data.

A number of measured gamma spectra were studied in order to derive three library spectra. All of the high resolution

laboratory or in the field. In order to make this a manageable problem, some limitations and assumptions had to be incorporated.

First of all, the source spectra are transported through air only, and not through such materials as might be found in a real transport problem. Secondly, the detector counting times are determined so as to give a predetermined spectral intensity, whereas in reality, this flexibility may not exist. Thirdly, the theoretical detector has a collecting area of one square centimeter, and is equally sensitive to all energy groups. Finally, it must always be remembered that the Finite Elements Method itself is only an approximation of the transport solution, not an exact (analytic) solution.

The assumptions made in this problem are outlined in detail in chapter 3, which discusses the transport phenomena.

#### LAYOUT OF CHAPTERS

The chapters are organized in the order of the subjects presented in this introduction. Chapter 2 begins with the selection of the sources, chapter 3 covers the transport of the sources, and chapter 4 completes the solution with a detailed presentation of Bayes' theorem and the counting statistics. Chapter 5 discusses the results and compares them with the method of photopeak identification, and the last chapter outlines the conclusions and recommendations, including a discussion of the applications of this method to 'real world' scenarios.

of the ideal detector. Initially, the Poisson distribution will be used, under the assumption that all channels of the detector collect counts independently of each other (statistically independent). In order to test the sensitivity of the analysis, a multinomial distribution will be used instead of the Poisson distribution, this time under the assumption that the detector channels are statistically interdependent.

Finally, the fourth part of this thesis problem entails writing a subroutine which uses Bayes' theorem to examine the transported spectra at any given distance from the source and output the probability that a particular spectrum is that of "Source A" given the transported spectrum. This is repeated for all sources (Source B, etc.) for the measured spectrum at a number of ranges and the results plotted. The Bayesian source likelihoods can be determined at ranges beyond the acceptable limits (to be defined in chapter V) of photopeak identification, and the utility of the Bayes' theorem method will be assessed. The computer code(s) for the third and fourth parts of this thesis will be combined as one and written in the BASIC computer language and run on an Apple II series computer.

### Limitations

This problem is designed to verify a theoretical technique using numerical methods. As such, the thesis does not pretend to duplicate all the constraints found in a

photopeak analysis fails. In so doing, it will be shown that information about the source can be gained from the downscattered photons.

#### Approach

The problem will be broken down into four main parts. First, a set of realistic 'generic' source spectra will be developed based on the gamma ray spectra of isotopes likely to be found in a nuclear source. A number of different sources will be developed in order to test the ability of Bayes' probability theory to discriminate between different nuclear sources.

The second part of the problem involves developing a computer program to transport each individual source spectrum for any distance through the atmosphere. The first thesis done on this topic attempted to transport gamma ray spectra using Monte Carlo techniques (7). This method proved to be far too cumbersome for the given problem and will not be investigated further. Instead, this thesis will use multigroup diffusion theory, which should be a more applicable transport technique (8). The multi-group diffusion code developed here uses the Finite Elements Method with a one-dimensional spherical coordinate geometry and will be written in Fortran 77 on the AFIT/AD Harris 800 minicomputer.

The third major effort will be to incorporate a subroutine to analyze the counting statistics at the location

where  $F$  is now the function that minimizes the penalty function  $P$  (3). Next,  $F$  is replaced by  $F + \delta F$ , where  $\delta F$  is arbitrarily small, and equation (3) becomes

$$P(F + \delta F) = \frac{1}{2} \int dV \{ D \nabla (F + \delta F) \cdot \nabla (F + \delta F) + \Sigma^a (F + \delta F)^2 - 2(F + \delta F)S \} \quad (4)$$

By multiplying through and collecting terms on the right hand side, equation (4) becomes

$$P(F + \delta F) = P(F) + \int dV \{ D \nabla \delta F \cdot \nabla F + \Sigma^a F \delta F - \delta F S \} + O(\delta^2 F) \quad (5)$$

The terms of order  $\delta^2 F$  in equation (5) can be neglected, as they are vanishingly small, so that the equation is of the form

$$P(F + \delta F) = P(F) + P(\delta F) \quad (6)$$

$$\text{or} \quad \delta P = P(F + \delta F) - P(F) \quad (7)$$

In order to obtain the smallest penalty, the right hand side of equation (7) must go to zero. From equations (5) and (7) then

$$\delta P = \int dV \{ D \nabla \delta F \cdot \nabla F + \Sigma^a F \delta F - \delta F S \} \quad (8)$$

By using integration by parts and Stoke's theorem, the

incremental penalty function becomes

$$\delta P = \int dV \delta F \{ -\underline{\nabla} \cdot (D \underline{\nabla} F) + \Sigma^a F - S \} \quad (9)$$

This results in a final form of  $\delta P$ , given by

$$\delta P = \int d\mathbf{a} \delta F D \underline{\nabla} F + \int dV \delta F \{ -\underline{\nabla} \cdot (D \underline{\nabla} F) + \Sigma^a F - S \} \quad (10)$$

Therefore, to minimize this quantity ( $\delta P$ ), both of the integrands (one surface and one volume) must go to zero.

$$\underline{\nabla} F = 0 \quad (11)$$

$$-\underline{\nabla} \cdot (D \underline{\nabla} F) + \Sigma^a F - S = 0 \quad (12)$$

It is evident from the results presented in equations (11) and (12) that the penalty function given by equation (3) accurately describes the diffusion problem (comparing equations (1) and (12)). Now the problem has been reduced to one of minimizing the penalty function in equation (3) by solving for the function  $F$ .

#### Digitizing the Problem.

The methodology discussed above must now be worked into a form conducive to computer implementation. The finite element nature of the problem enters when the function  $F$  is represented by a homogeneous cubic polynomial function. In one dimension, this function is given by equation (13) (top of next page):

$$F(l_1, l_2) = \sum_{i=1}^4 z_i f_i(l_1, l_2) \quad (13)$$

The values of  $z$  are the fluxes and currents (flux derivatives) at the mesh boundaries, and hence represent the ultimate form of the solution of the finite element problem. The functions  $f_i$  in equation (13) are expressed in terms of the natural coordinates  $l_1$  and  $l_2$ .

$$l_1 + l_2 = 1 \quad (14)$$

In addition,  $l_1$  has a value of 1 at the left mesh node and 0 at the right node, whereas  $l_2$  is 0 on the left and one on the right. The mesh configuration is illustrated in figure 2 below.

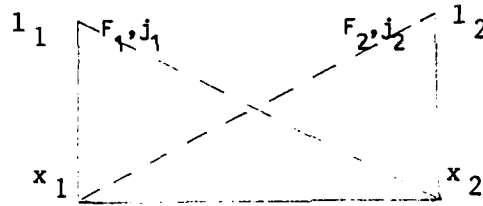


Figure 2. One-Dimensional Version of  $F(l_1, l_2)$   
The function  $F$  in equation (3) has now been approximated in terms of the mesh quantities  $F_1, j_1, F_2, j_2$ ; the fluxes and currents at the nodal points. In its expanded form equation (13) becomes

$$F = F_1 f_1(l_1, l_2) + j_1 f_2(l_1, l_2) + F_2 f_3(l_1, l_2) + j_2 f_4(l_1, l_2) \quad (15)$$

The cubic polynomial functions are given by the following equations

$$f_1 = l_1^3 + 3l_1^2 l_2 \quad (16)$$

$$f_2 = -\frac{h}{D} l_1^2 l_2 \quad (17)$$

$$f_3 = l_2^3 + 3l_1 l_2^2 \quad (18)$$

$$f_4 = \frac{h}{D} l_1 l_2^2 \quad (19)$$

Equation (3) can now be expressed in terms of the function  $F$  in equation (15). Both the first and second terms in equation (3) can be replaced with the aid of equations (16) - (19). For instance, the second term in equation (3) becomes

$$\frac{1}{2} \int dl \Sigma^a \{ F_1 f_1 + j_1 f_2 + F_2 f_3 + j_2 f_4 \}^2 \quad (20)$$

Equation (20) can be expanded and the integral evaluated by using the integral formula given in the equation below (15).

$$\int dl (l_1^p l_2^q) = \frac{h p! q!}{(p+q+1)!} \quad (21)$$

The first term in equation (3) is done in a similar fashion, with the additional aid of the relationships

$$dl_1/dx = -1/h \quad (22)$$

$$dl_2/dx = 1/h \quad (23)$$



The third term in equation (3) is approximated using Simpson's integral approximation, since the value of the source function  $S$  can be calculated throughout the region of interest (5).

Once the three terms in equation (3) have been approximated, it is a simple matter to get it into a form which allows for computer coding. All three integral terms have been put in a form allowing for evaluation over the interval of interest, and equation (3) becomes

$$P = \frac{1}{2} \underline{z} \cdot \underline{M} \cdot \underline{z} - \underline{z} \cdot \underline{S} - \tilde{\lambda} (\underline{c} \cdot \underline{z} - \underline{d}) \quad (24)$$

The first term is simply a combination of the first two integral terms in equation (3), having been expanded and combined into a single matrix  $M$ . This global matrix is a combination of all the local matrices, there being one local matrix for each mesh space used. Recall that the local matrices were obtained by evaluating terms one and two of equation (3) using equations (16) - (20).

The  $S$  matrix consists of the values of the third integral term in equation (3), which was evaluated using Simpson's Rule. The last term in equation (24) was added to account for the boundary conditions of the problem.

Finally, the  $z$  matrix is an array containing the values of the flux and current at each node. Hence, the problem remains to solve for the values of the  $z$  matrix by minimizing

equation (24). By taking the partial derivative of P in equation (24) with respect to z and setting it equal to zero, as well as the partial derivative of M with respect to  $\lambda$ , a series of linear equations is obtained. The equations, expressed in matrix form are rearranged and ultimately used to solve for the z matrix

$$\underline{z} = \underline{M}^{-1}\underline{S} + \underline{M}^{-1}\underline{c}_1\tilde{\lambda}_1 + \underline{M}^{-1}\underline{c}_2\tilde{\lambda}_2 \quad (25)$$

The transport code is written to solve just this set of equations.

#### The One-Dimensional, Single Group Problem.

As a first step to running the transport code using the Finite Element Method, a simple case was programmed. This case involves a one dimensional "slab geometry" problem with a known source function S, and a known fluence solution (12). The diffusion equation for this geometry becomes:

$$-D\left(\frac{dF(x)}{dx}\right)^2 + \Sigma^a F(x) = S(x) \quad (26)$$

and the final equation for the penalty function becomes

$$P = \frac{1}{2} \int_b^a dx \left( D\left(\frac{dF}{dx}\right)^2 + \Sigma^a F^2 - 2FS \right) \quad (27)$$

This is precisely the problem which was derived in the last section, using the one-dimensional cubic polynomials

(equation 15). Since the fluence as a function of distance is already known, it becomes an easy matter to check the results of the program.

The program was tested on the case where the fluence and source functions are given by

$$F(x) = x^4 \quad (28)$$

$$S(x) = -12x^2 + x^4 \quad (29)$$

The finite element solution (using the source function) is graphed along with the actual solution in figure 3.

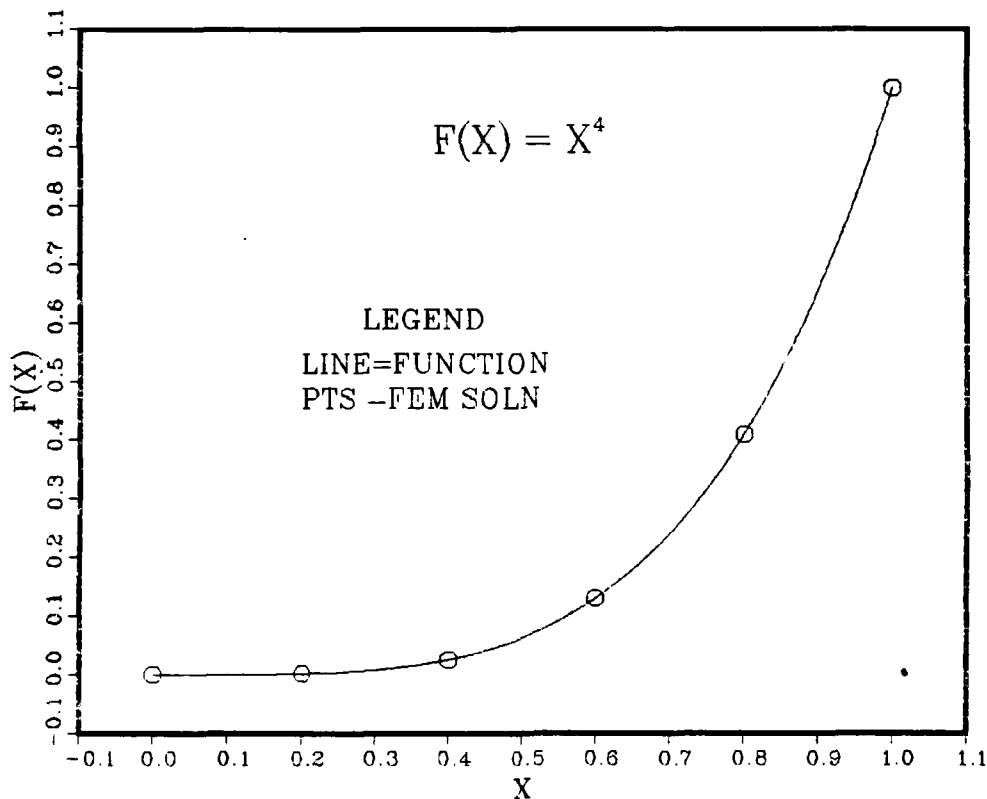


Figure 3. Finite Elements Solution Verification

As can be seen in figure 3, the match provided by the Finite Elements Method is very good indeed.

#### The Three-Dimensional, Multi-Group Problem.

Following the code verification in one dimension, it is necessary to expand the code into the three-dimensional (spherical geometry) multigroup problem. Since assumption number (5) assumes radial symmetry, the only dependence is on the variable  $r$ . As is explained in appendix C, the three-dimensional problem can be placed into a form which allows the use of the one-dimensional approximating polynomials, given by equations (15) - (19). Hence the problem needs only to be modified to accept the multiple energy groups.

The transition from single to multigroup is very straight-forward. The program is modified to calculate the solutions for flux and current on the nodes (the  $z$  matrix) one time for each group. This involves setting up the global matrix once for each group as well as modifying the source term used in the Simpson's approximation. Beginning with the highest energy group (group 1), the diffuse fluence solution is due only to inscattering of the uncollided photons. As the program solves each consecutively lower energy group, the source term is modified to account for the downscattered fluence from higher energy groups as well as the inscattered contribution. The iterative process proceeds in the direction of decreasing energy groups, and hence upscattering from lower energy groups to higher energy groups is not

allowed.

In order to verify the full scale radiation transport code, a known function similar to equations (28) and (29) was input, only in this case it was a simple exponential function. Again, the code output values are very close to the actual solution. A more important bench mark is attained by solving the diffusion equation analytically for a simple case. The analytic solution is outlined in appendix D, along with the value returned by the transport code. As can be seen in appendix D, the answer is acceptable, given only a one meshspace approximation.

#### Source Transport

The next step in the process is the actual transport of each library source to the desired ranges. Each of the sources was reconstructed at the desired ranges, yielding a degraded set of source spectra due to scattering and absorption losses. The two types of transported sources are discussed below.

#### The Measured Spectra

In order to simulate measured spectra at various ranges from the sources, it is necessary to transport the library spectra in two different fashions. The first method involves using the transport code (developed above) alone to determine the relative intensities of each library spectrum at a number of different ranges. These spectra represent the ideal measured spectra, since the transport code does not introduce

any random processes or counting statistics by itself. These "reference spectra" thus represent good data sets which would be obtained from an enormous number of measurements in the field (i.e., the true mean in each channel).

The second method involves taking the reference (ideal) spectra mentioned above and converting each one into a measured spectrum by introducing random counting statistics. The statistics subprogram introduces random variations in the counting data in line with the appropriate statistical distribution. Two different distributions will be employed in deriving the measured source spectra: the Poisson distribution and the multinomial distribution. Since the measured sources are actually generated during the analysis part of the problem, the methodology will be covered in detail in chapter IV and its appendices.

There are now two different sets of spectra which will be used in the analysis process. The first set consists of a good group of measured spectra; the "reference spectra," which was obtained by the transport of the library spectra. These reference spectra are equivalent to a set of spectra determined by many different measurements of the sources. The reference sources have been plotted out at ranges of 50, 100, 200, 300, 400 and 500 meters, and are presented in figures 4 through 9. It is important to note that the reference source spectra are in  $4\pi r^2$  fluence units, so they can be easily compared with the library sources. The actual values of fluence for the reference sources are tabulated in

tables III-1 through III-6.

The second set of source spectra represents a less than ideal group of spectra; the "measured spectra," obtained by the transport of the library spectra with the addition of counting statistics considerations. This group is equivalent to a set of spectra obtained by taking a single measurement of the sources. Since the measured sources are generated during the analysis process, they will be listed in chapter IV.

#### Background Considerations

In addition to the reference spectra and measured spectra discussed above, the library spectra were generated a third time, but this time background counts were accounted for. The background spectrum provided with the high resolution data was used to determine the mean number of background counts present in each channel of the reference source spectra. The measured source spectra are generated in a manner similar to the "no background case," but now a separate subroutine is used to generate random background counts in line with the appropriate statistics. These background counts are then added, channel by channel, to the measured source spectrum of interest. Again, the generation of the measured source spectra is discussed at length in chapter IV.

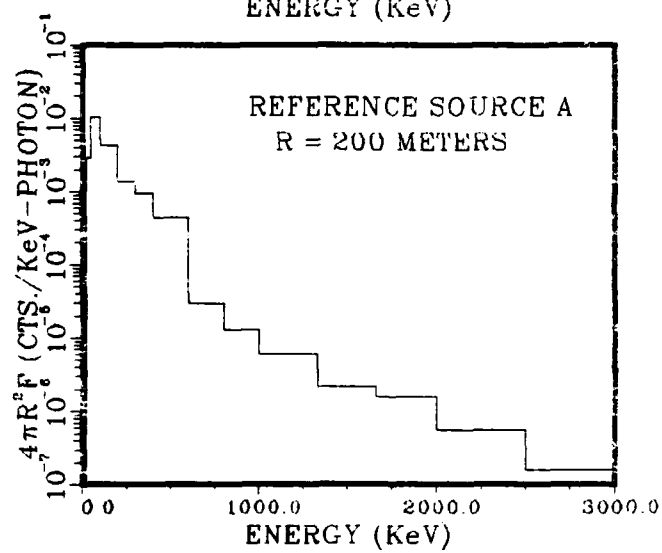
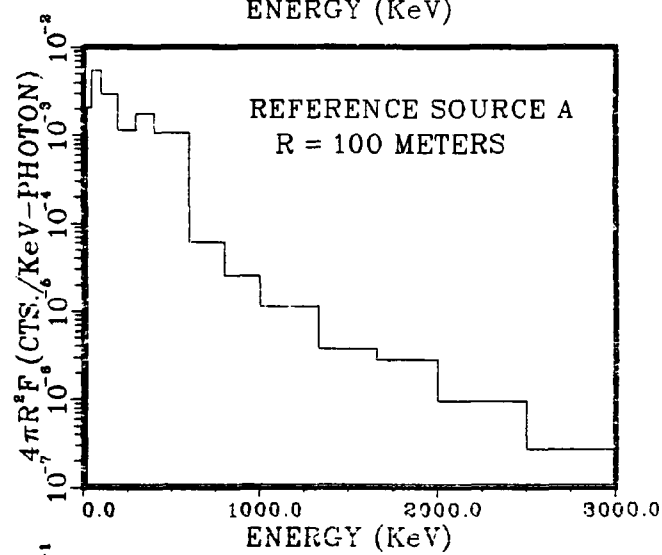
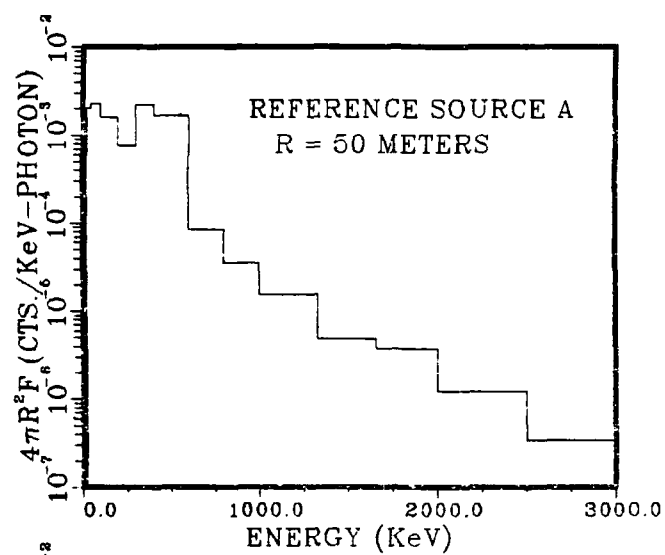


Figure 4. Reference Source A at 50, 100 & 200 meters



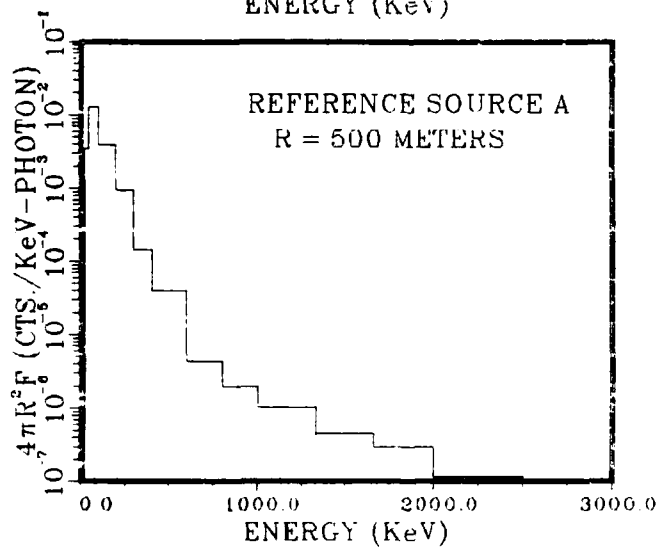
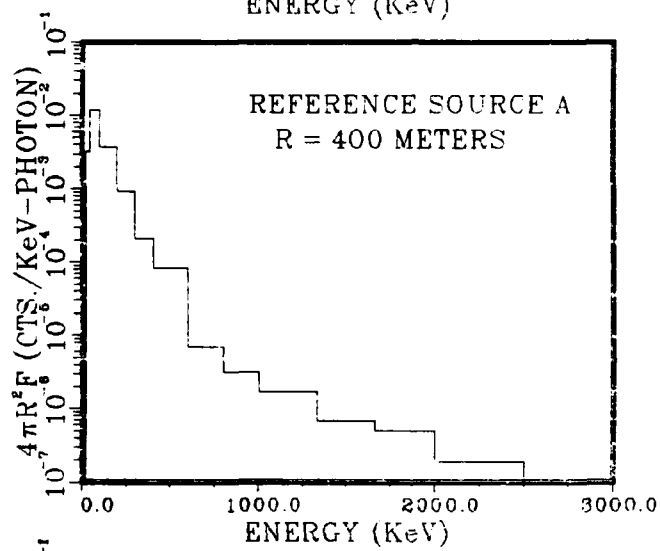
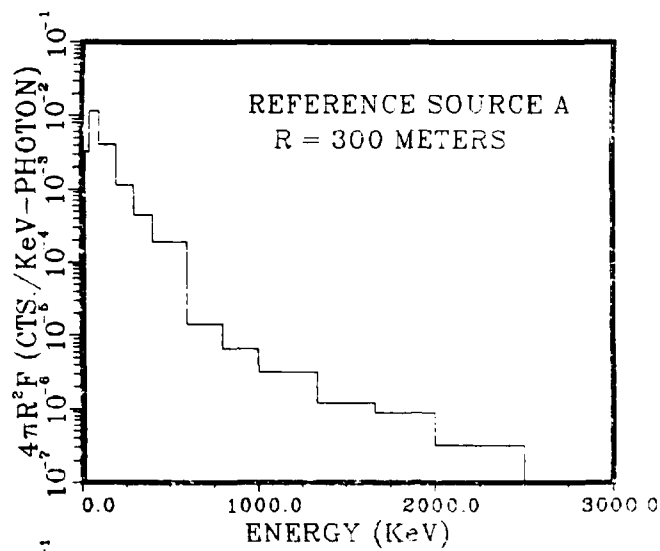


Figure 5. Reference Source A at 300, 400 & 500 meters

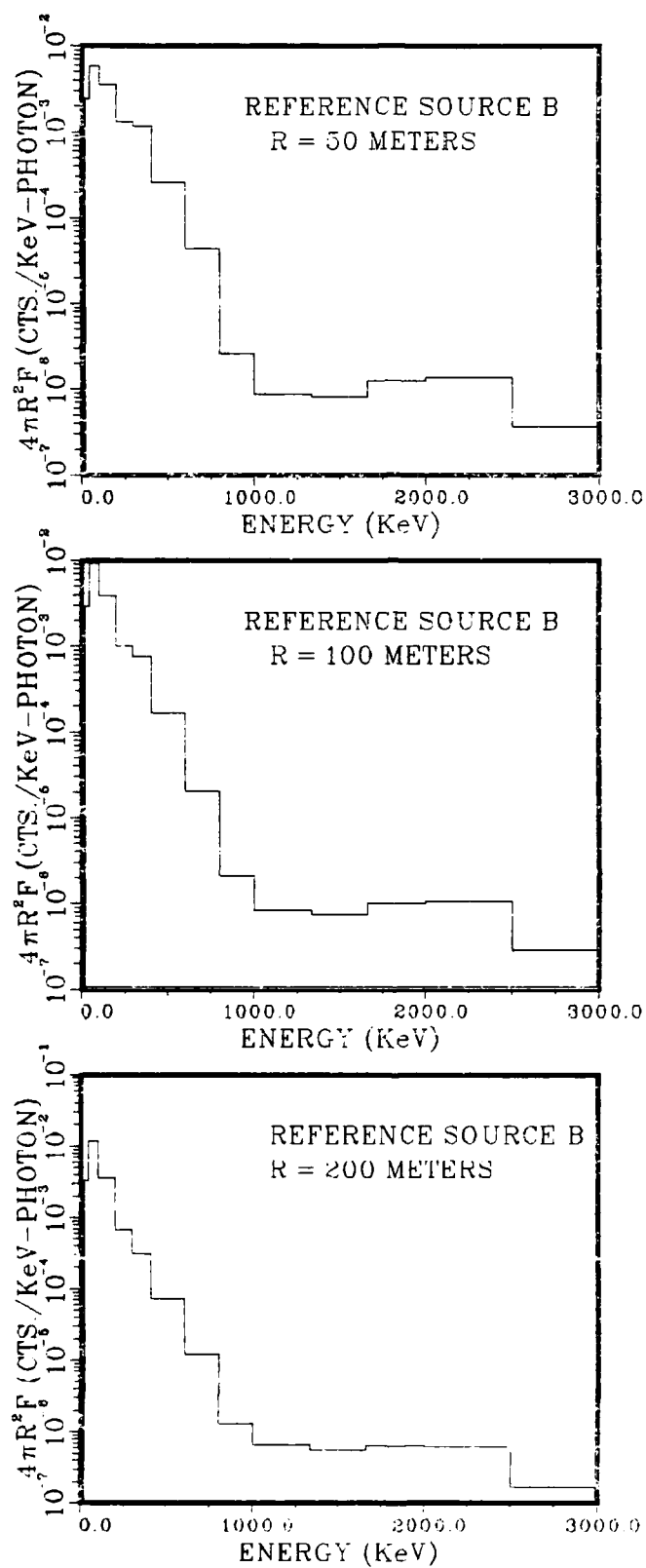


Figure 6. Reference Source B at 50, 100 & 200 meters

Table IV-1: Sample Prior Distribution

<u>Source</u>	<u>Number in Sample</u>	<u>P(A<sub>i</sub>)</u>
1	5	0.5
2	2	0.2
3	3	0.3

The second term in the numerator of equation (30),  $P(X|A_i)$ , is the probability of obtaining the measured spectrum  $X$  given the reference spectrum  $A_i$ . This term is a calculated quantity, and will vary depending on the type of counting statistics used.

#### Poisson Distribution.

The first method of determining the values of  $P(X|A_i)$  will assume that the counts are collected in a Poisson distribution. The assumption then is that each one of the eighteen channels in the low resolution detector is statistically independent from the others. The Poisson distribution is a particularly valid one in counting problems when the average number of counts is much smaller than the total possible number (i.e., smaller than the number of gamma photons emitted by the entire nuclear source) (4). Counting data collected in a Poisson distribution is obtained by running the detector for an arbitrary length of time, which generally yields a different number of total counts each time. This is in contrast to the multinomial distribution, which will be covered later in this chapter.

represents the prior distribution of the three different sources. As a starting point, the three values will be assumed equal, with

$$P(A1) = 0.3333 \quad (33)$$

$$P(A2) = 0.3333 \quad (34)$$

$$P(A3) = 0.3333 \quad (35)$$

In other words, it is assumed that each of the three sources occurs equally often. This quantity can be varied to test the sensitivity of the posterior distribution. In the case of actual source measurements in the field, the prior distribution would presumably be known.

As a simple example of the prior distribution, assume ten containers of nuclear materials have had the identifying labels removed. Further, assume that the only way to determine the identity of the nuclear material in each of the containers is to measure the spectrum of each with a multichannel gamma-ray detector at a range of 100 meters. In order to use Bayes' Theorem, the prior distribution must be determined. In this example problem, the total number of each type of material is known, so it is a simple matter to determine the prior distribution, as seen in table IV-1. In the main thesis problem, it is assumed that the prior distribution is also a given.

which is the joint probability of the variables  $X$  and  $A_i$  (17). Or, in other words

$$P(A_i, X) = P(X, A_i) \quad (32)$$

The denominator in equation (30) is the sum of all the combined likelihood functions and prior distributions. The summation is over the total number of reference sources, which is three in this problem.

As can be seen in equation (30), Bayes' theorem allows for the combination of prior information (the prior distribution of sources) and the measured data (the likelihood functions) to determine the posterior distribution, given by  $P(A_i|X)$ . The posterior distribution gives the probability (likelihood) of having source  $A_i$ , given the measured spectrum  $X$ . For a given measured source  $X$ ,  $P(A_1|X)$  is the probability that the source  $A_1$  is actually the one being measured. The power of this method is that it clearly allows for the combination of all available information in arriving at the posterior distribution.

#### Applied Form

Having reviewed Bayes' Theorem in its general form, the next task is to examine it specifically in relation to this problem. The equation will be examined term by term, and the specific quantities will be identified as they apply to this problem.

As was mentioned above, the  $P(A_i)$  term in equation (30)

$$P(A_i|X) = \frac{P(X|A_i) P(A_i)}{\sum_{j=1} P(X|A_j) P(A_j)} \quad (30)$$

The variable  $A_i$  (where  $i = 1, 3$ ) represents the known data, or in this case, the reference sources, and  $X$  represents the given sample data, or the measured source. Therefore,  $P(A_i)$  is the probability of occurrence of the reference source  $A_i$ . Quite simply,  $P(A_i)$  represents the proportion of occurrence of source  $A_i$ , so that if there exists a group of ten nuclear sources, of which four are known to be of type  $A_1$  and six of type  $A_2$ , then  $P(A_1) = 0.40$  and  $P(A_2) = 0.60$ . This probability distribution is defined as the "prior distribution." The prior distribution is the unconditional probability of  $A_i$  occurring.

Given that  $X$  represents the observed or measured value of a source, then the  $P(X|A_i)$  term in equation (30) is the probability that the measured source spectrum  $X$  is due to the reference spectrum  $A_i$ . Given the source spectrum  $A_1$  then,  $P(X|A_1)$  is the probability that a measured spectrum  $X$  is caused by the spectrum  $A_1$ . This probability is defined as the likelihood function, and is a discrete value in this problem, since there is a predefined number of sources. Note that the numerator in equation (30) can also be expressed as

$$P(A_i, X) = P(X|A_i) P(A_i) \quad (31)$$

#### IV. Identification and Analysis of Source Spectra

In chapter II, the library source spectra were derived, and the methodology for creating the reference spectral sources and the measured spectral sources was described. In chapter III, the transport code was developed using the Finite Element Method (FEM). This code was employed to generate the reference source spectra discussed in chapter III. Now that all the raw data is available, a technique must be defined by which the measured sources can be identified and analyzed. The methods of identification and analysis will be discussed in this chapter.

##### Bayes Theorem

###### General Form.

The method of identifying sources in this thesis will use Bayes' Theorem. In the general sense, the term Bayesian is used to describe an approach to combining information that uses the sample information (i.e., data collected) as well as other available information (17). In the case of spectral source identification, the sample information consists of the measured spectra, and the other information is the set of reference spectra.

Bayes' theorem allows one to make an assessment of the likelihoods of the occurrence of certain events, given the sample information. In terms of the variables  $X$  and  $A$  (top of next page):

TABLE III-6

Relative Intensity Distribution of Reference Source C  
(counts / photon)

<u>Group Number</u>	<u>300 meters</u>	<u>400 meters</u>	<u>500 meters</u>
1	0.0	0.0	0.0
2	0.0	0.0	0.0
3	0.0	0.0	0.0
4	0.0	0.0	0.0
5	0.0	0.0	0.0
6	2.78E-15	9.35E-16	3.58E-16
7	1.45E-14	4.73E-15	1.81E-15
8	2.28E-14	7.23E-15	2.84E-15
9	1.02E-14	3.96E-15	2.29E-15
10	3.37E-14	1.07E-14	4.66E-15
11	1.75E-14	6.23E-15	3.43E-15
12	3.54E-14	1.17E-14	5.81E-15
13	1.29E-13	4.04E-14	1.90E-14
14	1.52E-13	4.51E-14	2.18E-14
15	1.14E-12	3.36E-13	1.54E-13
16	1.69E-11	6.31E-12	3.15E-12
17	4.00E-11	1.62E-11	9.24E-12
18	6.75E-12	2.73E-12	1.58E-12



TABLE III-5

Relative Intensity Distribution of Reference Source C  
(counts / photon)

<u>Group Number</u>	<u>50 meters</u>	<u>100 meters</u>	<u>200 meters</u>
1	0.0	0.0	0.0
2	0.0	0.0	0.0
3	0.0	0.0	0.0
4	0.0	0.0	0.0
5	0.0	0.0	0.0
6	3.61E-13	6.98E-14	1.04E-14
7	2.02E-12	3.85E-13	5.61E-14
8	3.40E-12	6.43E-13	9.14E-14
9	2.37E-13	1.08E-13	3.05E-14
10	5.23E-12	9.76E-13	1.37E-13
11	5.42E-13	2.31E-13	5.81E-14
12	4.76E-12	9.22E-13	1.39E-13
13	2.67E-11	4.55E-12	5.60E-13
14	2.76E-11	5.08E-12	6.75E-13
15	3.56E-10	5.55E-11	5.71E-12
16	1.29E-9	3.00E-10	5.67E-11
17	1.31E-9	4.49E-10	1.17E-10
18	3.41E-10	8.99E-11	2.02E-11

TABLE III-4  
Relative Intensity Distribution of Reference Source B  
(counts / photon)

<u>Group Number</u>	<u>300 meters</u>	<u>400 meters</u>	<u>500 meters</u>
1	0.0	0.0	0.0
2	0.0	0.0	0.0
3	0.0	0.0	0.0
4	0.0	0.0	0.0
5	0.0	0.0	0.0
6	4.49E-15	1.51E-15	5.80E-16
7	1.60E-14	5.29E-15	2.06E-15
8	1.15E-14	3.91E-15	1.77E-15
9	1.04E-14	3.76E-15	1.95E-15
10	1.30E-14	4.85E-15	2.65E-15
11	1.33E-14	4.45E-15	2.23E-15
12	9.46E-14	2.39E-14	8.04E-15
13	5.84E-12	1.53E-13	5.60E-14
14	1.14E-12	2.71E-13	1.01E-13
15	3.97E-12	1.59E-12	9.56E-13
16	2.45E-11	1.05E-11	6.19E-12
17	4.54E-11	2.08E-11	1.30E-11
18	7.53E-12	3.46E-12	2.12E-12

TABLE III-3

Relative Intensity Distribution of Reference Source B  
(counts / photon)

<u>Group Number</u>	<u>50 meters</u>	<u>100 meters</u>	<u>200 meters</u>
1	0.0	0.0	0.0
2	0.0	0.0	0.0
3	0.0	0.0	0.0
4	0.0	0.0	0.0
5	0.0	0.0	0.0
6	5.84E-13	1.13E-13	1.69E-14
7	2.20E-12	4.21E-13	6.18E-14
8	1.36E-12	2.72E-13	4.29E-14
9	8.49E-13	1.94E-13	3.58E-14
10	9.15E-13	2.18E-13	4.29E-14
11	1.67E-12	3.32E-13	5.12E-14
12	2.78E-11	4.53E-12	4.88E-13
13	1.63E-10	2.67E-11	2.94E-12
14	3.75E-10	6.00E-11	6.22E-12
15	4.15E-10	8.07E-11	1.33E-11
16	1.12E-9	3.06E-10	7.12E-11
17	9.38E-10	3.74E-10	1.17E-10
18	2.34E-10	7.05E-11	1.96E-11

TABLE III-2  
Relative Intensity Distribution of Reference Source A  
(counts / photon)

<u>Group Number</u>	<u>300 meters</u>	<u>400 meters</u>	<u>500 meters</u>
1	0.0	0.0	0.0
2	0.0	0.0	0.0
3	0.0	0.0	0.0
4	0.0	0.0	0.0
5	0.0	0.0	0.0
6	4.16E-15	1.40E-15	5.37E-16
7	1.41E-14	4.65E-15	1.82E-15
8	2.64E-14	8.33E-15	3.23E-15
9	3.55E-14	1.13E-14	4.78E-15
10	9.16E-14	2.75E-14	1.10E-14
11	1.13E-13	3.14E-14	1.25E-14
12	2.54E-13	6.97E-14	2.80E-14
13	3.31E-12	8.08E-13	2.56E-13
14	3.96E-12	1.05E-12	4.56E-13
15	1.02E-11	4.64E-12	2.98E-12
16	3.65E-11	1.85E-11	1.25E-11
17	5.23E-11	2.94E-11	2.06E-11
18	8.55E-12	4.81E-12	3.37E-12

TABLE III-1

Relative Intensity Distribution of Reference Source A  
(counts / photon)

<u>Group Number</u>	<u>50 meters</u>	<u>100 meters</u>	<u>200 meters</u>
1	0.0	0.0	0.0
2	0.0	0.0	0.0
3	0.0	0.0	0.0
4	0.0	0.0	0.0
5	0.0	0.0	0.0
6	5.41E-13	1.05E-13	1.57E-14
7	1.92E-12	3.69E-13	5.42E-14
8	4.02E-12	7.56E-13	1.07E-13
9	5.04E-12	9.70E-13	1.42E-13
10	1.60E-11	2.92E-12	3.91E-13
11	2.23E-11	4.03E-12	5.15E-13
12	5.37E-11	9.51E-12	1.19E-12
13	1.05E-9	1.68E-10	1.76E-11
14	7.03E-10	1.37E-10	1.85E-11
15	2.40E-10	8.97E-11	2.67E-11
16	5.14E-10	2.35E-10	8.41E-11
17	3.56E-10	2.15E-10	1.03E-10
18	1.93E-10	4.87E-11	1.72E-11

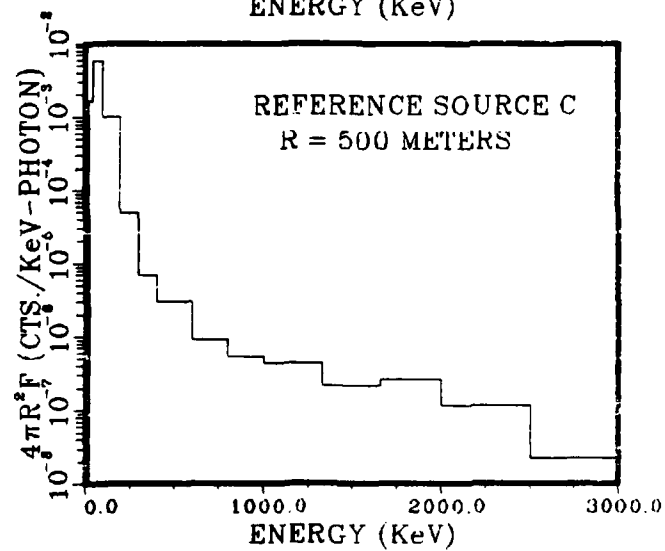
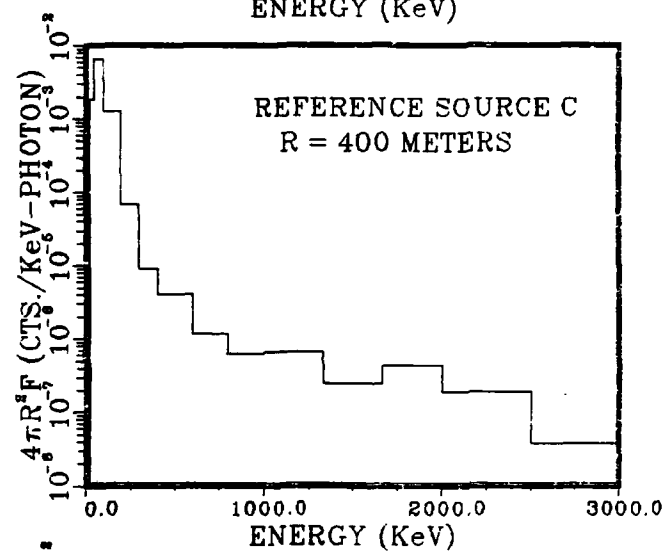
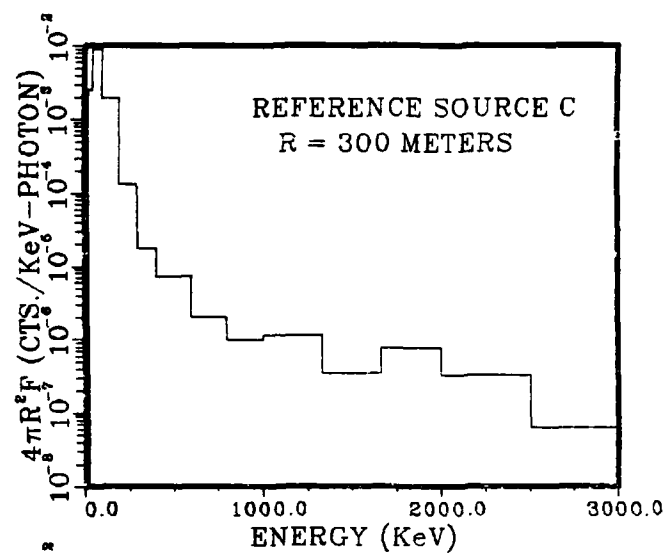


Figure 9. Reference Source C at 300, 400 & 500 meters

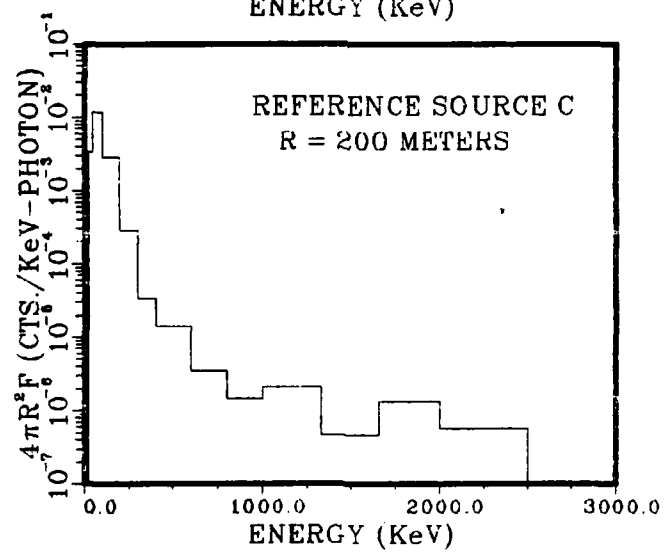
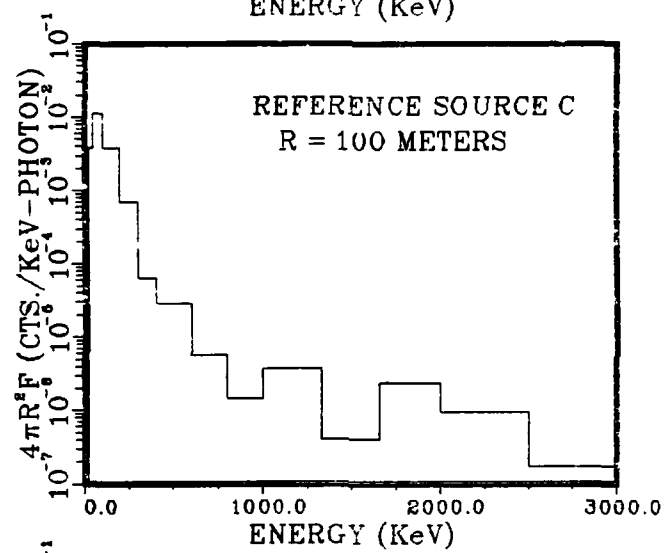
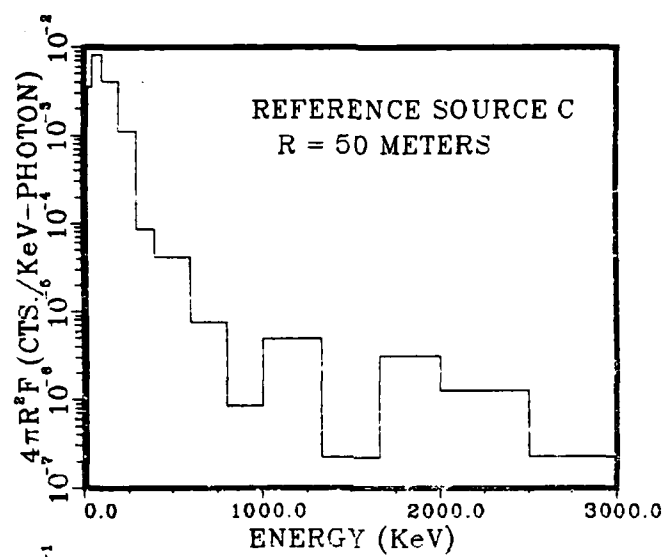


Figure 8. Reference Source C at 50, 100 & 200 meters

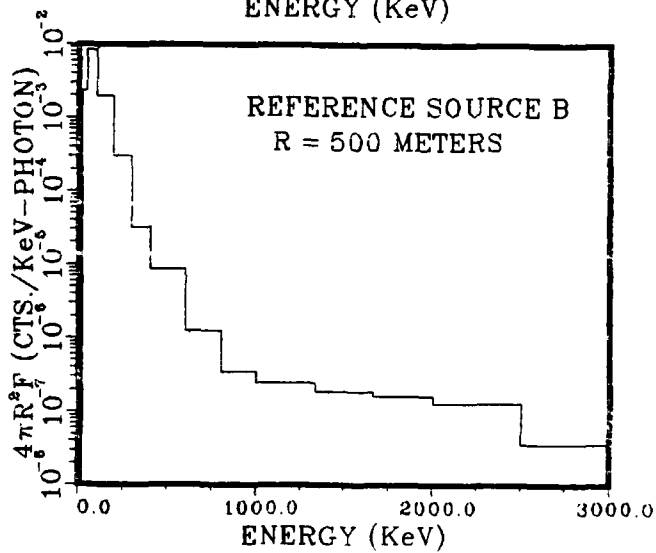
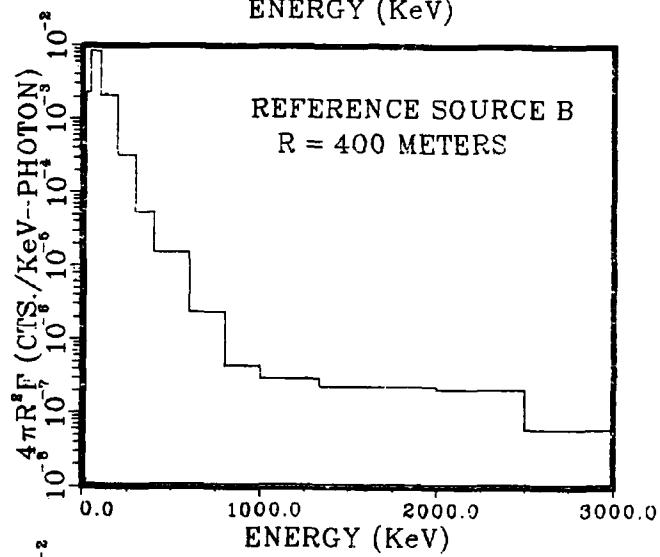
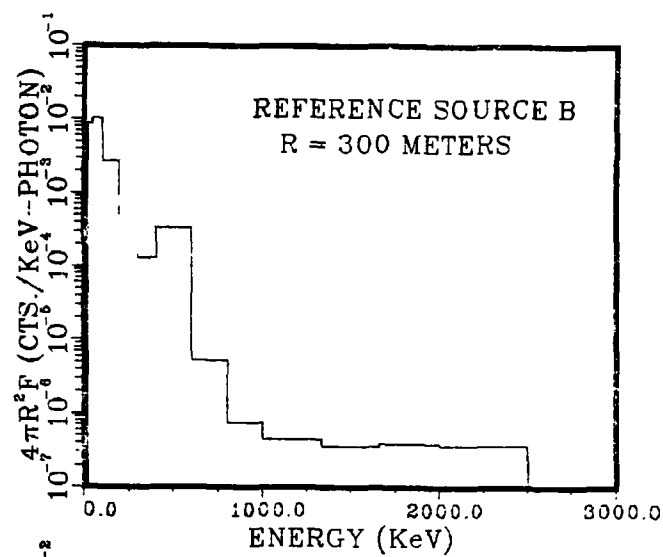


Figure 7. Reference Source B at 300, 400 & 500 meters



The Poisson distribution is given by

$$P(x, a) = \frac{a^x}{x!} \exp(-a) \quad (36)$$

where the variable  $a$  is the mean number of counts occurring in the channel of interest, and  $x$  is the observed number of counts in the channel (4). Or, in the case of a multichannel detector, equation (36) becomes

$$P(x_k, a_{ik}) = \frac{(a_{ik})^{x_k}}{x_k!} \exp(-a_{ik}) \quad (37)$$

where  $k$  denotes the channel number, which ranges from one to eighteen. In order to get an expression for  $P(X|A_i)$ , the individual channel probabilities must be combined into a single probability. This is achieved by noting that since the channels are statistically independent of one another, the probabilities multiply. Hence the relationship becomes

$$P(X|A_i) = \prod_{k=1}^{18} \frac{(a_{ik})^{x_k}}{x_k!} \exp(-a_{ik}) \quad (38)$$

The mean number of counts in channel  $k$  is given by  $a_{ik}$ , and comes from the reference spectrum, discussed in chapter III (ref. figures 4 - 9). The final form of equation (38) then becomes (top of next page):

$$P(X|A_i) = \prod_{k=1}^{18} \frac{(\bar{S}_{ik} + \bar{B}_k)^{x_k}}{x_k!} \exp(-(\bar{S}_{ik} + \bar{B}_k)) \quad (39)$$

Here  $\bar{S}_{ik}$  represents the mean number of counts from reference spectrum  $i$  ( $i = 1, 3$ ) in channel number  $k$  ( $k = 1, 18$ ) and  $\bar{B}_k$  is the mean number of background counts in channel  $k$ . Recall that initially, the analysis is done with zero background counts in all channels of all sources.  $X_k$  in equation (39) represents the number of counts in channel  $k$  observed in the measured spectrum.

The Poisson version of the Bayes' theorem analysis was coded in the BASIC computer language and run on an Apple II series computer. The program listing and description is included in appendix H.

The value of  $X_k$ , obtained from the measured source spectrum, is obtained using a random number generator and the Poisson distribution. Details of this process are covered in appendix G. On the other hand, the values of  $S_{ik}$  come from the reference source spectra, which were discussed in chapter III. The method of obtaining numerical values for the reference sources is discussed in appendix F.

#### Gaussian Distribution.

In the limit of a large number of counts, the Poisson distribution approaches the normal or Gaussian distribution, which is given by (top of next page):

$$P(X|A_i) = \prod_{k=1}^{18} \frac{\exp(-\frac{1}{2}(x_k - (\bar{S}_{ik} + \bar{B}_k))/\sigma_{ik}))}{(2\pi\sigma_{ik}^2)^{\frac{1}{2}}} \quad (40)$$

Here,  $\sigma_{ik}$  is the standard deviation of the counts of source  $i$  in channel  $k$ . The standard deviation squared is therefore equal to the number of counts observed in the channel of interest,  $X_k$ . All other terms in equation (40) are defined the same as in the Poisson distribution.

In practice (in this problem) the Gaussian distribution is used anytime the counts measured in any one channel exceed 34, since the factorial in the denominator of the Poisson distribution (equation (39)) exceeds the overflow limits of the computer (1E+38). The Gaussian version of the Bayes' theorem analysis was also coded in BASIC, and is included in appendix H.

A new measured source spectrum is generated each time the analysis code is run, and hence determines the values for  $X_k$  in equation (40). The method of obtaining a measured source spectrum with a Gaussian distribution is contained in appendix G. The method of obtaining reference source spectra is the same as in the Poisson version.

#### Multinomial Distribution.

The second main method of performing the Bayes' theorem analysis employs the multinomial distribution. Unlike the Poisson (and Gaussian) distribution, the counts in the different channels of a multinomial distribution are all

interdependent (2). To obtain a multinomial distribution in a multichannel analyzer, counts are collected until a certain predetermined total is reached, at which time the detector is turned off. By collecting in this manner, the number of counts collected in one channel becomes dependent on the counts in all other channels (10). This dependence follows quite simply because each count collected in one channel decreases by one the total counts available for all other channels. In terms of equation (30) variables, the multinomial distribution is given as

$$P(X|A_i) = \frac{N!}{\prod_{k=1}^{18} x_k!} \prod_{k=1}^{18} (f_{ik})^{x_k} \quad (41)$$

Here  $X_k$  again represents the measured number of counts in channel  $k$ , subject to the constraint

$$\sum_{k=1}^{18} x_k = N \quad (42)$$

where  $N$  is the the total number of counts in all channels combined (13). The variable  $f_{ik}$  is the fraction of the counts of source  $i$  occurring in channel  $k$ . The  $f_{ik}$ 's are obtained from the reference source spectra and the methodology is discussed at length in appendix F. The  $f_{ik}$  values are subject to the constraint

$$\sum_{k=1}^{18} f_{ik} = 1 \quad (43)$$

for each source.

As was true in the Poisson and Gaussian analysis codes, the multinomial analysis code is contained in appendix H. The method of obtaining the measured source ( $X_k$ ) is discussed in appendix G, and the reference sources ( $f_{ik}$ ) in appendix F.

## V. Results and Discussion

Having the reference sources in hand, the problem remains to analyze the measured sources at the ranges of 50, 100, 200, 300, 400 and 500 meters from the source. The sections in this chapter will be presented in order of the analysis runs. First the Bayes' theorem analysis is done using Poisson statistics with no background contribution. Secondly, the multinomial version of Bayes' theorem is used, again with no background. Thirdly, the Poisson version will be run again, but this time using the background contribution discussed earlier. Finally, an unknown source will be "measured" in one pass at a distance of 50 meters, to see how the Bayes' posterior distribution behaves with a nonlibrary source spectrum.

### Bayes' Theorem With Poisson: No Background

The Bayes analysis code using the Poisson statistics package was run at all ranges using each of the three sources as a measured source once at each range. Hence, this constituted 18 runs using the Poisson and Gaussian codes (depending on the level of counts, ref. chapter IV). The baseline level of counts was assigned as 1000 counts at 50 meters. This corresponds to a collecting time of approximately 30 minutes, using the one square centimeter detector assumed in this problem. An equal counting time was assumed for each measurement, in line with Poisson counting

statistics. The total number of reference counts in each source and the measured source values for each run were determined as discussed in appendices F and G.

The results of the posterior distribution are presented in table V-1. As can be seen in the posterior distribution for measured source A, the probability of positively identifying the measured source drops below the 99.7% level near the 200 meter mark, but stays above 70% all the way out to 500 meters. Measured sources B and C do not stay above the 70% level, although source C remains well above the 90% level out to 400 meters. Part of the reason for the consistently high values with source A is because of the relative strength of the source. As can be seen in table V-3, measured source A has a total of 20 counts collected, which is twice the number of counts in both sources B and C at 500 meters. This follows because library source A has more high energy features relative to sources B and C, and high energy photons are degraded less severely than are low energy photons (reference cross section data in appendix B).

When comparing these results to the method of photopeak identification (reference appendix A), it is evident that the uncollided photons are rapidly degraded by the exponential scattering term, and the peaks soon drop below the 3 sigma level. As can be seen in appendix A, the characteristic photopeak of source B has already degraded below the 3 sigma level at 50 meters, and the photopeaks of sources A and C drop below 3 sigma shortly beyond 50 meters. Therefore,

Table V-1  
Bayes' Posterior Distribution  
(Poisson with no background)

1. Measured: Source A

<u>RANGE (m)</u>	<u>P(A1 X)</u>	<u>P(A2 X)</u>	<u>P(A3 X)</u>
50	1.000	0.000	0.000
100	1.000	9.081E-21	0.000
200	9.913E-1	8.660E-3	7.707E-5
300	8.780E-1	1.192E-1	2.800E-3
400	7.810E-1	1.891E-1	2.989E-2
500	7.396E-1	2.113E-1	4.908E-2

2. Measured Source B

<u>RANGE (m)</u>	<u>P(A1 X)</u>	<u>P(A2 X)</u>	<u>P(A3 X)</u>
50	0.000	1.000	0.000
100	0.000	1.000	1.626E-6
200	6.926E-8	8.671E-1	1.329E-1
300	8.519E-2	8.049E-1	1.099E-1
400	7.682E-3	4.599E-1	5.324E-1
500	1.862E-3	4.192E-1	5.790E-1

3. Measured Source C

<u>RANGE (m)</u>	<u>P(A1 X)</u>	<u>P(A2 X)</u>	<u>P(A3 X)</u>
50	0.000	0.000	1.000
100	0.000	0.000	1.000
200	5.543E-25	2.310E-4	9.998E-1
300	7.065E-5	8.319E-2	9.167E-1
400	2.834E-7	7.390E-2	9.261E-1
500	1.396E-2	4.919E-1	4.942E-1



Table V-2  
Measured Source A (Poisson Distribution)

channel	50 m	100 m	200 m
<u>number</u>	<u>counts</u>	<u>counts</u>	<u>counts</u>
1	0	0	0
2	0	0	0
3	0	0	0
4	0	2	0
5	0	0	0
6	0	0	0
7	1	1	1
8	3	0	1
9	3	0	1
10	6	1	1
11	8	1	1
12	17	2	0
13	332	54	5
14	222	44	5
15	77	28	9
16	162	73	26
17	113	69	32
18	60	16	5

Table V-3  
Measured Source A (Poisson Distribution)

channel	300 m	400 m	500 m
<u>number</u>	<u>counts</u>	<u>counts</u>	<u>counts</u>
1	1	0	0
2	1	0	1
3	1	0	1
4	0	0	0
5	0	1	0
6	0	1	1
7	1	1	2
8	0	1	0
9	0	0	1
10	0	0	0
11	0	0	0
12	1	1	0
13	2	0	1
14	1	0	0
15	3	1	2
16	12	6	3
17	19	10	7
18	3	2	1

Table V-4  
Measured Source B (Poisson Distribution)

channel	50 m	100 m	200 m
<u>number</u>	<u>counts</u>	<u>counts</u>	<u>counts</u>
1	0	0	0
2	1	1	1
3	1	0	1
4	0	0	0
5	0	0	0
6	1	1	1
7	3	0	2
8	1	1	0
9	1	0	1
10	0	1	0
11	1	0	0
12	7	2	0
13	50	6	2
14	114	18	1
15	127	25	5
16	341	94	21
17	287	114	36
18	71	21	6

Table V-5  
Measured Source B (Poisson Distribution)

channel	300 m	400 m	500 m
<u>number</u>	<u>counts</u>	<u>counts</u>	<u>counts</u>
1	1	0	1
2	0	0	0
3	0	1	0
4	0	2	0
5	1	0	1
6	0	1	0
7	1	0	0
8	0	0	0
9	1	0	0
10	0	1	0
11	1	0	2
12	0	1	0
13	2	0	0
14	1	1	1
15	2	0	0
16	7	4	1
17	13	4	4
18	2	1	0

Table V-6  
Measured Source C (Poisson Distribution)

channel	50 m	100 m	200 m
<u>number</u>	<u>counts</u>	<u>counts</u>	<u>counts</u>
1	1	1	0
2	0	1	1
3	0	1	0
4	0	1	0
5	1	0	0
6	0	0	1
7	0	0	1
8	1	1	0
9	0	0	0
10	0	0	0
11	2	0	0
12	1	0	0
13	7	2	2
14	9	2	0
15	106	16	0
16	382	89	18
17	389	134	35
18	101	29	5

Table V-7  
Measured Source C (Poisson Distribution)

channel	300 m	400 m	500 m
<u>number</u>	<u>counts</u>	<u>counts</u>	<u>counts</u>
1	0	0	0
2	0	0	1
3	2	1	0
4	0	1	0
5	0	0	0
6	1	0	1
7	0	0	1
8	0	0	0
9	0	0	0
10	0	2	0
11	0	0	0
12	1	0	0
13	0	1	2
14	0	0	0
15	0	0	0
16	6	1	2
17	13	5	3
18	2	0	0

eventually the probability in equation (40) becomes zero (exceeding the computer limits of  $1E-38$ ). This leads to a zero term in the denominator of equation (30) of chapter IV, leaving an undefined Bayes' posterior distribution. This problem is even more likely to occur at higher count levels, that is, in regions close to the source where photopeak identification is at its best. Hence, when the Bayes' theorem method yields "undefined" probabilities, it serves as an indicator that an unknown source, that is, a source not in the library, has been encountered. Other methods must then be used to determine the composition of the new source.

#### Applying the Results

What can be learned from these results that can be applied to experiments in the field? First of all, it appears from the contrast between the Poisson and multinomial statistics that it is far better to run the detector as long as possible in order to optimize the number of counts (Poisson). If the detector is automatically shut off after reaching a certain number of counts, much information is lost from the stronger sources. This effect was observed in the Poisson runs without background. Indeed, even though all of the sources used in this analysis were assumed to be of equal strength, a slight statistical increase in the number of counts (source A) was significant in terms of positive identification.

Another point of interest uncovered in the analysis is

Table V-13

## Measured Source C

(Poisson Distribution with Background)

channel

<u>number</u>	<u>50 m</u>	<u>100 m</u>	<u>200 m</u>	<u>300 m</u>	<u>400 m</u>	<u>500m</u>
1	2	4	1	1	1	2
2	0	1	0	0	0	0
3	1	0	0	0	2	2
4	2	0	0	1	2	0
5	1	0	0	2	0	1
6	1	3	2	3	4	0
7	6	6	6	5	4	6
8	7	3	4	7	5	6
9	21	19	23	22	20	22
10	24	23	22	26	23	24
11	241	242	242	241	240	240
12	23	21	25	22	26	24
13	48	41	41	40	40	41
14	46	40	41	40	41	40
15	167	77	64	61	61	62
16	529	237	162	151	148	145
17	472	217	117	94	83	83
18	140	66	43	39	39	40



Table V-12  
Measured Source B  
(Poisson Distribution with Background)

channel						
<u>number</u>	<u>50 m</u>	<u>100 m</u>	<u>200 m</u>	<u>300 m</u>	<u>400 m</u>	<u>500m</u>
1	3	1	2	1	1	0
2	1	0	1	3	1	0
3	0	0	0	1	1	2
4	2	1	0	0	0	1
5	2	2	0	1	2	1
6	0	1	4	1	7	3
7	5	5	5	5	5	6
8	5	5	4	4	5	5
9	22	20	23	21	20	19
10	24	23	22	23	24	22
11	240	242	241	243	241	240
12	31	24	24	22	22	23
13	90	50	41	44	42	39
14	153	56	39	39	39	40
15	192	88	63	62	60	61
16	488	241	168	150	149	149
17	370	197	115	94	87	86
18	111	59	45	41	38	38

Table V-11  
Measured Source A  
(Poisson Distribution with Background)

channel						
<u>number</u>	<u>50 m</u>	<u>100 m</u>	<u>200 m</u>	<u>300 m</u>	<u>400 m</u>	<u>500m</u>
1	1	1	0	2	1	0
2	0	0	1	0	0	1
3	1	1	0	0	1	2
4	1	1	0	0	1	2
5	0	0	3	1	1	0
6	0	3	3	1	1	0
7	5	7	5	5	5	1
8	6	5	4	7	5	7
9	24	22	19	24	22	21
10	29	26	24	23	23	24
11	249	240	240	240	241	241
12	40	26	21	23	22	23
13	372	94	47	42	43	42
14	262	83	45	39	40	39
15	139	91	67	64	62	61
16	309	220	174	158	152	151
17	194	149	116	96	90	88
18	101	54	43	41	38	38

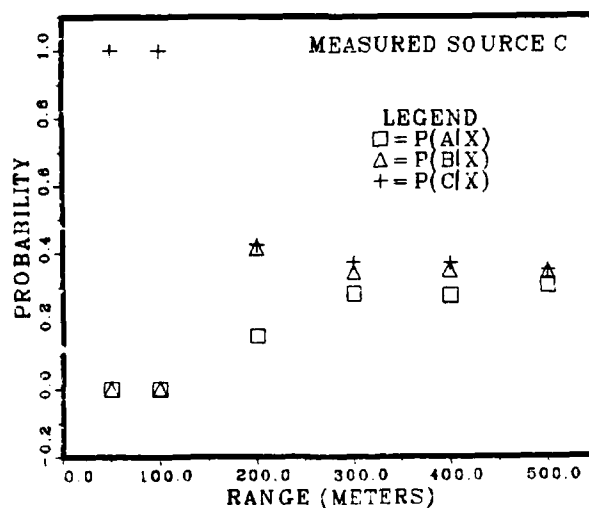
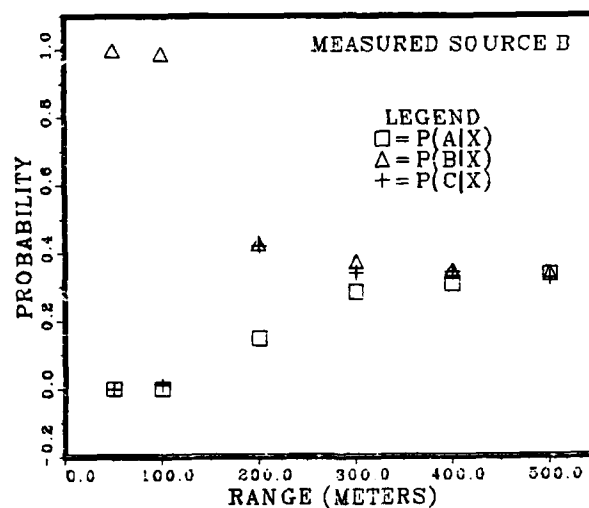
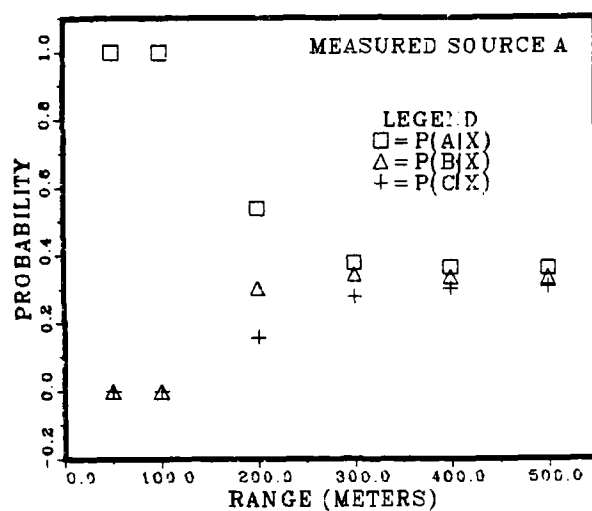


Figure 12. Posterior Distributions: Poisson with Background

Table V-10

## Bayes' Posterior Distribution

(Poisson with background)

1. Measured: Source A

<u>RANGE (m)</u>	<u>P(A1 X)</u>	<u>P(A2 X)</u>	<u>P(A3 X)</u>
50	1.000	0.000	0.000
100	1.00	7.463E-11	4.244E-19
200	5.384E-1	3.026E-1	1.591E-1
300	3.783E-1	3.424E-1	2.793E-1
400	3.642E-1	3.339E-1	3.019E-1
500	3.611E-1	3.319E-1	3.070E-1

2. Measured Source B

<u>RANGE (m)</u>	<u>P(A1 X)</u>	<u>P(A2 X)</u>	<u>P(A3 X)</u>
50	0.000	1.000	0.000
100	8.479E-15	9.886E-1	1.140E-2
200	1.488E-1	4.297E-1	4.215E-1
300	2.841E-1	3.739E-1	3.420E-1
400	3.104E-1	3.464E-1	3.432E-1
500	3.368E-1	3.380E-1	3.252E-1

3. Measured Source C

<u>RANGE (m)</u>	<u>P(A1 X)</u>	<u>P(A2 X)</u>	<u>P(A3 X)</u>
50	0.000	0.000	1.000
100	0.00	1.691E-3	9.983E-1
200	1.571E-1	4.182E-1	4.247E-1
300	2.814E-1	3.447E-1	3.739E-1
400	2.764E-1	3.514E-1	3.722E-1
500	3.060E-1	3.442E-1	3.499E-1

probabilities for positive source identification degrade much more rapidly than in the case with no background. All three sources maintain high probabilities of positive identification out to 100 meters, at which time the background level overwhelms the number of source counts. But as can be seen in tables V-11 - V-13, the source counts in each channel are already becoming obscured by background at 100 meters (compare with tables V-2 - V-7). In cases with a large amount of background then, Bayes' theorem appears to lose information quite rapidly, but still offers some improvement over the method of photopeak identification.

#### The Unidentified Source

One of the severe limitations of Bayes' theorem applied to spectral identification appears to be in the realm of identifying unknown sources, or sources simply not contained in the source library. When an unknown source was formulated which differed considerably from the library sources, the Poisson (Gaussian) analysis failed to return any numerical information whatsoever.

The problem is identified when examining equation (40) in chapter IV. When using the normal distribution (i.e., in a region of reasonable count levels), any excessive deviation from the reference value in a channel results in an extremely small value of  $P(X|A_i)$ , due to the exponential term. This problem is compounded if every one of the eighteen channels differs from each channel of the reference sources, since

Table V-9  
Relative Intensity and Count Levels of Background

<u>Channel</u>	<u>Counts/photon</u>	<u>Counts</u>
1	0.0	0.0
2	0.0	0.0
3	0.0	0.0
4	0.0	0.0
5	0.0	0.0
6	2.58E-3	1.29
7	1.01E-2	5.04
8	9.17E-3	4.59
9	4.18E-2	20.89
10	4.56E-2	22.82
11	3.64E-2	240.00
12	4.51E-2	22.56
13	8.11E-2	40.57
14	7.79E-2	38.95
15	1.21E-1	60.66
16	2.92E-1	145.96
17	1.61E-1	80.56
18	7.58E-2	37.91

### Bayes' Theorem With Poisson: With Background

In order to incorporate a background level into the Bayes' theorem analysis, it was necessary to generate a separate background "source" based on the high resolution data used to generate the original library sources (ref. chap. 2). The background measurements were taken at the same time the original source measurements were made, and therefore should accurately reflect the background in the low resolution detector of this problem. The relative intensity distribution of the background is presented in table V-9. A background level of 500 counts is assumed, based on the background measurements taken with a counting time of about 30 minutes (as before). The reference levels based on this number are also provided in table V-9. Since the Poisson distribution is being used, the background level will remain constant at each range (i.e., same counting time).

The reference level of counts was added channel by channel to each reference source spectrum, and a random (measured) background count level was determined separately using the same method as was discussed in appendix G. Hence the random number generator is called upon twice: once to generate the "normal" measured source spectrum, due to the photo emissions of the nuclear material, and once to generate the measured background spectrum. The results of both calculations are then combined to yield a final measured source spectrum for the analysis process.

As can be seen in table V-10 (and figure 12), the

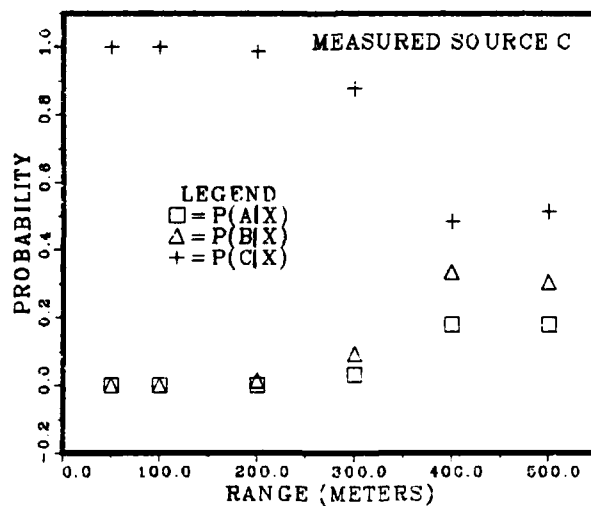
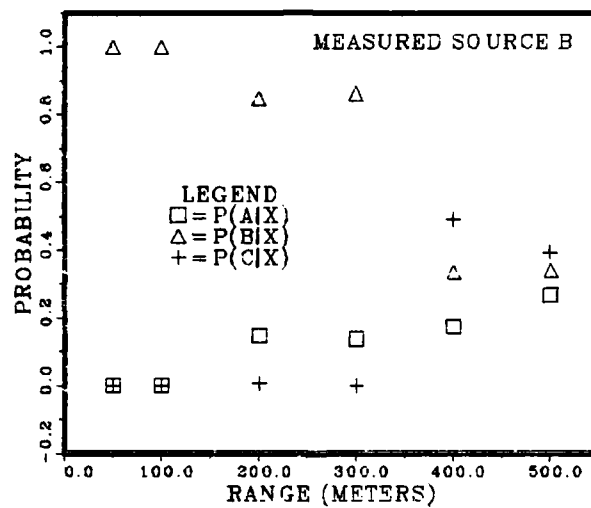
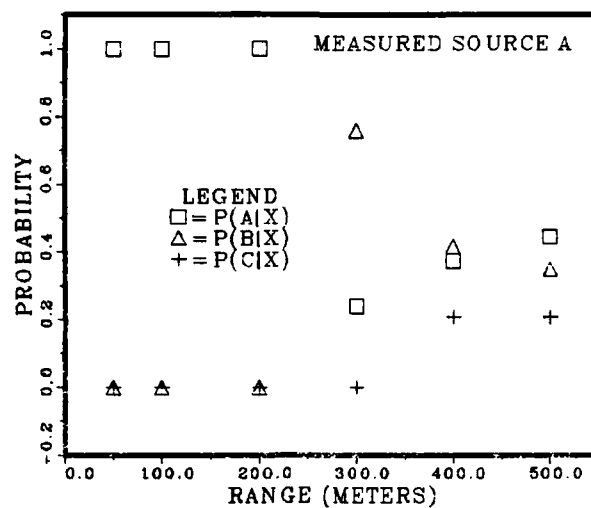


Figure 11. Posterior Distributions: Multinomial



Table V-8  
Bayes' Posterior Distribution  
(Multinomial with no background)

1. Measured: Source A

<u>RANGE (m)</u>	<u>P(A1 X)</u>	<u>P(A2 X)</u>	<u>P(A3 X)</u>
50	1.000	0.000	0.000
100	1.000	3.176E-30	0.000
200	9.999E-1	8.493E-5	1.101E-11
300	2.398E-1	7.586E-1	5.949E-4
400	3.743E-1	4.165E-1	2.092E-1
500	4.452E-1	3.483E-1	2.066E-1

2. Measured Source B

<u>RANGE (m)</u>	<u>P(A1 X)</u>	<u>P(A2 X)</u>	<u>P(A3 X)</u>
50	0.000	1.000	0.000
100	2.429E-29	1.00	3.852E-14
200	1.470E-1	8.468E-1	6.219E-3
300	1.378E-1	8.622E-1	1.453E-5
400	1.755E-1	3.344E-1	4.902E-1
500	2.673E-1	3.397E-1	3.930E-1

3. Measured Source C

<u>RANGE (m)</u>	<u>P(A1 X)</u>	<u>P(A2 X)</u>	<u>P(A3 X)</u>
50	0.000	0.000	1.000
100	0.000	5.675E-12	1.000
200	7.598E-8	1.349E-2	9.865E-1
300	3.223E-2	9.504E-2	8.727E-1
400	1.790E-1	3.355E-1	4.855E-1
500	1.798E-1	3.060E-1	5.142E-1

### Bayes' Theorem With Multinomial: No Background

As was discussed in chapter IV, the multinomial distribution is used when the detector counts to a predetermined number of counts, then shuts off. This method was programmed in order to contrast its effectiveness with that of the Poisson distribution, which has no constraint on the number of counts collected. The posterior distributions from the multinomial runs are presented in table V-8.

Even though the multinomial analysis was done using the same initial reference count level of 1000 counts at 50 meters, it can be seen that the probabilities of accurately identifying a measured source drop off much more drastically than do the Poisson values. The assumption that each source measured has exactly the same number of counts (the basis for this distribution) probably drives the values down more rapidly as the range increases. Recall in the case of Poisson statistics, source A had more total counts collected at 500 meters than did either of the other measured sources, which aided in maintaining a higher probability with increased range.

The results presented in table V-8 are also depicted graphically in figure 11. Since the multinomial distribution yields lower values of probability, the Poisson methodology will be used exclusively in the remaining analysis effort.

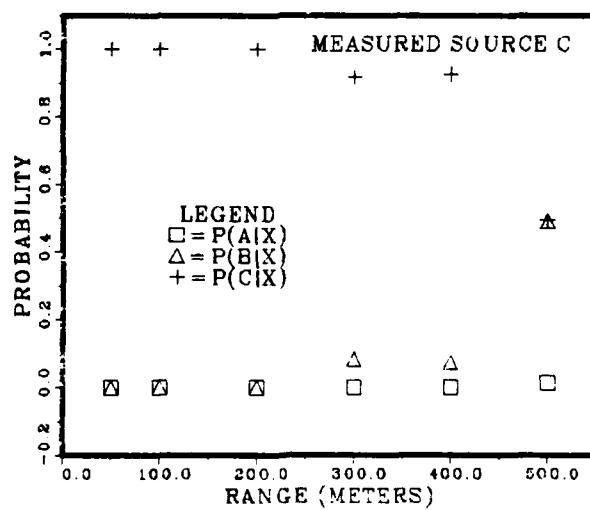
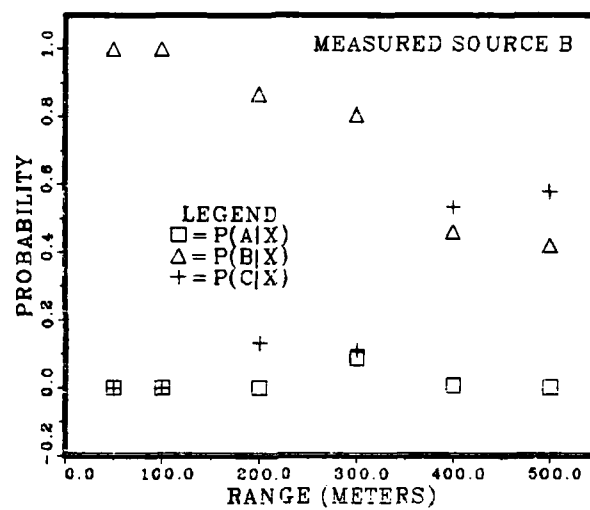
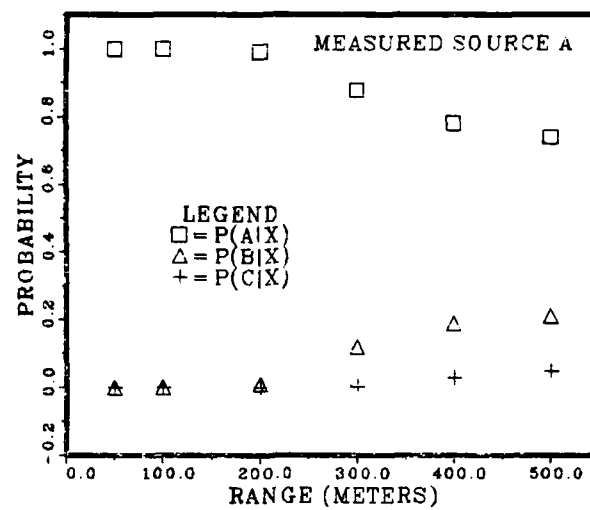


Figure 10. Posterior Distributions: Poisson

Bayes' theorem extends positive identification a minimum of 100 meters for sources A and C, and 50 meters for source B (reference table V.1).

The most striking aspect of the Bayes' probabilities is that they remain relatively high even though the number of counts available is very small. Indeed, all three source spectra look strikingly similar at 400 meters, yet measured source A is still identified 78.1% of the time, and measured source C 92.6% of the time. Therefore, if the criterion for positive identification is reduced to a level less than 3 sigma, Bayes' theorem can extend the range of identification even further.

This is in contrast to the method of photopeak identification, which fails at relatively small ranges (around 50 meters). This failure is due to the small number of uncollided photons available, since the number is rapidly reduced by the exponential term in Beer's Law (appendix A). Even large photopeaks cannot withstand the exponential losses in conjunction with the rising background level due to downscattered photons. Indeed, in regions where enough photons exist to render photopeak identification viable (close to the source), Bayes' theorem will also return favorable results, as evidenced by the 100% values at a range of 50 meters.

The results of the Poisson version of the Bayes' analysis are plotted in figure 10.

the inability of Bayes' theorem to generate information on non-library source composition. A possible solution to this problem might be to build up a vast number of library sources based on the gamma ray spectra of specific isotopes. When an unknown is encountered, the Bayes' analysis could be run using different combinations of the isotopic reference sources, until a reasonable posterior distribution is reached. The probability of occurrence,  $P(A_i)$ , could also be modified in order to reach a high degree of certainty. Chapter VI will briefly discuss some follow on recommendations based on this subject.

## VI. Summary and Recommendations

To summarize this thesis problem, the purpose was to test Bayes' theorem, in theory, as an aid to extending the range of positive identification of nuclear materials, using features in the characteristic gamma ray spectra. To achieve this goal, four basic steps were initiated, as covered in the first four chapters of this report. First, the library source spectra had to be selected, by studying available high resolution gamma ray spectra. These were then regrouped into a convenient, low resolution form for which macroscopic cross sections are available (18 groups). Secondly, a transport code was developed using the Finite Element Method to transport these library sources to any desired range, in order to come up with the reference sources, or in other words, the sources which might result from the ideal measurement of the source spectra at a distance. Third, the reference sources were degraded into simulated measured sources by applying various statistical distributions, which included the Poisson (and Gaussian) and the multinomial distributions. And lastly, the measured sources were analyzed using Bayes' theorem in order to assess the probability that each measured source would be correctly identified. The results were compared with the method of photopeak identification, to see if any improvements could be gained by using Bayes' theorem.

As can be seen by the results in chapter V, Bayes'

theorem has strong points and weak points. As was seen in the case of measured sources with the background extracted, Bayes' theorem offers a dramatic increase in the accuracy of identification when contrasted with photopeak identification. When background is not extracted from the measurements prior to analysis, the results are less convincing in the low count environment (i.e., measurements taken at extreme distances), but still offer an improvement over photopeak identification. The major disadvantage with Bayes' theorem appears to be the requirement for the measured sources to be contained as library sources in order to be identified.

#### Recommendations

Bayes' theorem does indeed extend the range of detection of nuclear materials, but much more research needs to be done. Some follow-on areas of research include investigating the utility of Bayes' theorem on high resolution data. Theoretically, the results should be even more dramatic than in the low resolution case. This is evident from equation (40) in chapter IV, where it is seen that the deviations between measured and reference (library) counts in channels will make the probability extremely small in the case of a mismatch, since the multiplication has increased from 18 channels to a much larger number of channels. Therefore, the probability of measuring the wrong source will approach a small number (possibly zero) much more rapidly than in the 18 channel scenario. An interesting follow-on effort could test

this concept by increasing the number of channels to some (arbitrary) large number. The 18 gamma group cross section data could be interpolated to accomodate this larger number of energy groups.

Secondly, a method should be investigated that can adjust the prior distribution in conjunction with the library sources in order to positively identify new sources. As was mentioned in chapter V, a large number of isotopic library sources might be developed and used in combination with the prior distribution to determine if Bayes' theorem can aid in identifying new sources. As it stands now, the results discussed in chapter V show that Bayes' theorem yields no information on new source composition, when only a small number of library sources is available. This aspect of Bayes' theorem is a potentially complicated problem, and unfortunately, time didn't allow it to be addressed in this effort.



## Appendix A: Photopeak Analysis Considerations

### Photopeak Analysis in Theory.

As has been mentioned in several places throughout the main text, the basic premise of this thesis is to extend the range of spectral identification by applying Bayes' theorem to measured spectra instead of the method of photopeak identification. The principal difference in these two methods is that photopeak identification uses only the uncollided fluence as an identification feature, whereas Bayes' theorem uses both the uncollided fluence and the scattered fluence as useful information for means of source identification.

Mathematically, the virgin (uncollided) fluence is attenuated exponentially, as is seen in Beer's Law:

$$I(r) = I_0(r) \exp(-\Sigma^t r) / 4 \pi r^2 \quad (44)$$

In equation (44),  $\Sigma^t$  is the total macroscopic cross section for interaction for photons at the given energy. Hence, any interaction, including absorption and scattering, removes a photon from the uncollided fluence category.

In order for a photopeak to be useful for source identification purposes, it must be a minimum of three standard deviations (sigma) above the background level. In the case of the Poisson distribution, one standard deviation is the square root of the number of counts in the given channel. A three sigma level provides a 99.73 percent certainty of positive

identification (4). Therefore, when a photopeak falls below the three sigma level, the method of photopeak identification is no longer reliable. Since Bayes' theorem uses a portion of the downscattered photons for identification purposes, it should in theory extend the range of source identification beyond the range where the photopeaks drop below the three sigma level.

#### Photopeak Analysis in Practice.

In this problem, the three sigma criterion must be evaluated at each range at which the Bayes' theorem analysis is being performed. This involves first selecting distinct photopeaks in each high resolution source which makes each source unique.

Each of the original high resolution sources was examined for one very distinct line for the purpose of comparison. In source A the line occurs in channel 10, in source B it occurs in channel 12, and in source C the "test" photopeak also appears in channel 12. These photopeaks were then degraded using the following assumptions:

- (1) the line occurs at the center of the low resolution channel;
- (2) the line is infinitesimally narrow, so that no photons can downscatter into the photopeak;
- (3) the background (continuum) in the low resolution bin is divided equally among all the high resolution channels present in the bin.

In order to examine the "best case" for the method of photopeak identification, the relative intensity of each of the photopeaks at the source is used to calculate the number of uncollided counts present in the photopeak at a range of 50 meters. The count levels in the low resolution channels are obtained from tables V.2 through V.7 (Poisson Distribution with no background). The number of counts in each photopeak is determined using Beer's Law. This number is then subtracted from the number of measured counts in the appropriate low resolution channel, and the rest of the counts are divided equally among the high resolution channels, giving a smooth background level in accordance with assumption (3) above. Figure 13 illustrates the relationship between the low resolution bin and the high resolution structure.

As can be seen in figure 13, as the range increases, the photopeak will degrade in accordance with Beer's Law and the relative background level will increase as photons downscatter into the bin from higher energy channels.

The analysis was performed on the three photopeaks discussed above, and the results are contained in table A-1.

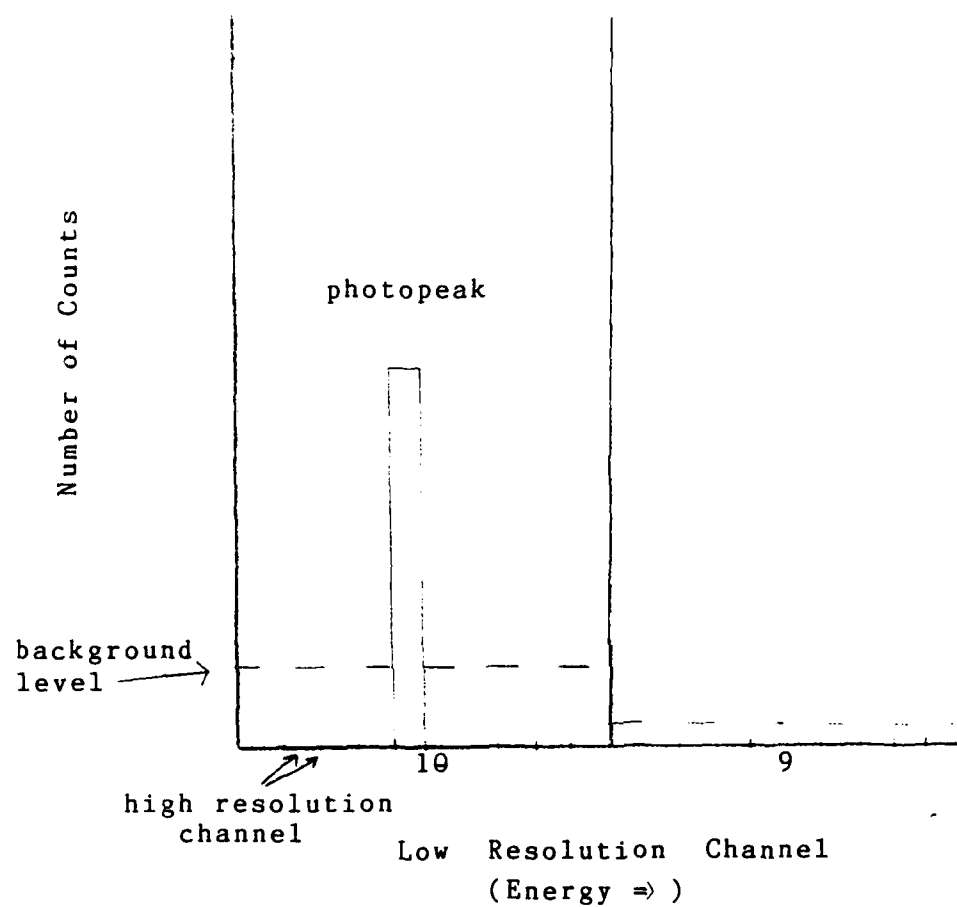


Figure 13. The High Resolution Bin Structure

TABLE A-1  
Photopeak Degradation

1. Source A

<u>COUNTS</u>	<u>50 meters</u>	<u>100 meters</u>	<u>200 meters</u>
total:	6.00	1.00	1.00
photopeak:	4.00	8.27E-9	3.87E-10
sigma:	2.39E-1	1.69E-1	1.69E-1
3 sigma:	7.17E-1	5.07E-1	5.07E-1
bkgd.:	5.71E-2	2.86E-2	2.86E-2

2. Source B

<u>COUNTS</u>	<u>50 meters</u>	<u>100 meters</u>	<u>200 meters</u>
total:	7.00	2.00	0
photopeak:	1.30	2.38E-9	0
sigma:	5.34E-1	3.16E-1	0
3 sigma:	1.60	9.49E-1	0
bkgd.:	2.85E-1	1.00E-1	0

3. Source C

<u>COUNTS</u>	<u>50 meters</u>	<u>100 meters</u>	<u>200 meters</u>
total:	1	0	0
photopeak:	1	0	0
sigma:	0	0	0
3 sigma:	0	0	0
bkgd:	0	0	0

## Appendix B: 18 Gamma Group Cross Sections

This appendix contains the data file listing of the 18 group sea level air gamma cross sections used in the radiation transport process. All cross sections are macroscopic, the units being inverse centimeters. The list begins with gamma group one (highest energy group) and continues down to group eighteen. The first two numbers in each group (separated by a comma) represent the group transport cross section and the group total cross section, in that order. The next value in each group is the cross section for scatter from group one into the current group. The next cross section is the scatter from group two, and so on, until within group scatter, which is the last cross section in each group (14).

2.6781E-5,3.0663E-5      (Group 1, 8000 - 10000 KeV)

1.2991E-6

2.9082E-5,3.3578E-5      (Group 2, 6500 - 8000 KeV)

2.1316E-6

1.5056E-6

3.0430E-5,3.7458E-5      (Group 3, 5000 - 6500 KeV)

2.2584E-6

3.2793E-6

2.3603E-6

3.4609E-5,4.2309E-5      (Group 4, 4000 - 5000 KeV)

1.6760E-6

2.3213E-6  
3.4861E-6  
2.5878E-6  
3.5861E-5, 4.8296E-5 (Group 5, 3000 - 4000 KeV)  
1.9585E-6  
2.6055E-6  
3.7052E-6  
5.6385E-6  
4.2018E-6  
4.4473E-5, 5.4819E-5 (Group 6, 2500 - 3000 KeV)  
1.1661E-6  
1.5069E-6  
2.0530E-6  
2.9597E-6  
4.6506E-6  
3.4867E-6  
4.5947E-5, 6.1097E-5 (Group 7, 2000 - 2500 KeV)  
1.3771E-6  
1.7477E-6  
2.3140E-6  
3.2071E-6  
4.7851E-6  
7.3590E-6  
5.1337E-6  
5.2539E-5, 6.8224E-5 (Group 8, 1660 - 2000 KeV)  
1.1220E-6  
1.4045E-6

1.8185E-6

2.4386E-6

3.4698E-6

5.0735E-6

7.4414E-6

5.3179E-6

5.3610E-5, 7.5903E-5 (Group 9, 1330 - 1660 KeV)

1.3140E-6

1.6295E-6

2.0759E-6

2.7143E-6

3.7127E-6

5.1831E-6

7.2570E-6

1.0756E-5

7.6158E-6

5.1254E-5, 8.6398E-5 (Group 10, 1000 - 1330 KeV)

1.6733E-6

2.0597E-6

2.5888E-6

3.3107E-6

4.3618E-6

5.8008E-6

7.6914E-6

1.0725E-5

1.5861E-5

1.2197E-5



6.1939E-5,9.8011E-5 (Group 11, 800 - 1000 KeV)

1.8052E-6

1.6008E-6

1.9948E-6

2.5154E-6

3.2290E-6

4.1378E-6

5.2363E-6

6.8793E-6

9.4990E-6

1.5564E-5

1.2529E-5

5.4339E-5,1.1023E-4 (Group 12, 600 - 800 KeV)

1.6878E-6

2.0662E-6

2.5674E-6

3.2143E-6

4.0659E-6

5.0889E-6

6.2289E-6

7.7982E-6

1.0093E-5

1.5022E-5

2.5010E-5

1.9937E-5

3.2786E-5,1.2779E-4 (Group 13, 400 - 600 KeV)

1.5137E-5

1.3442E-5  
1.1976E-5  
1.0767E-5  
9.9962E-6  
9.7302E-6  
1.0069E-5  
1.1029E-5  
1.2672E-5  
1.6497E-5  
2.3561E-5  
3.8612E-5  
3.6189E-5  
4.9010E-5, 1.4714E-4      (Group 14, 300 - 400 KeV)  
1.7477E-6  
2.1519E-6  
2.6905E-6  
3.3851E-6  
4.2817E-6  
5.3081E-6  
6.3437E-6  
7.5724E-6  
8.9861E-6  
1.1101E-5  
1.3958E-5  
1.8611E-5  
3.5381E-5  
3.7459E-5

AD-A159 244

IDENTIFICATION OF NUCLEAR MATERIALS FROM REMOTE  
DETECTION OF CHARACTERIST (U) AIR FORCE INST OF TECH  
WRIGHT-PATTERSON AFB OH SCHOOL OF ENGI L W BRASURE  
MAR 85 AFIT/GNE/PH/85M-2 F/G 18/4

2/2

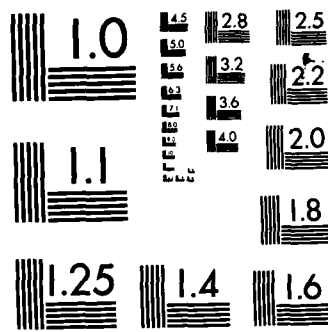
UNCLASSIFIED

NL

END

FILMED

DTIC



MICROCOPY RESOLUTION TEST CHART  
NATIONAL BUREAU OF STANDARDS-1963-A

1.7734E-5,1.6655E-4 (Group 15, 200 - 300 KeV)

1.1719E-6

1.5017E-6

1.9791E-6

2.6574E-6

3.6515E-6

4.9480E-6

6.4615E-6

8.5184E-6

1.1264E-5

1.6018E-5

2.2300E-5

2.7297E-5

3.6680E-5

6.4487E-5

6.4947E-5

5.2605E-5,1.9710E-4 (Group 16, 100 - 200 KeV)

0

0

0

0

0

0

0

0

0

0

6.5306E-7

5.7746E-6

1.9534E-5

4.5196E-5

1.0160E-4

1.4823E-4

1.4686E-4, 2.4089E-4 (Group 17, 50 - 100 KeV)

0

0

0

0

0

0

0

0

0

0

0

0

0

0

0

4.8024E-5

2.0558E-4

3.6340E-4, 4.0987E-4 (Group 18, 20 - 50 KeV)

0

0

0

0

0

0

0

0

0

0

0

0

0

0

0

0

2.5660E-5

2.5174E-4

## Appendix C: Simplifying the Three-Dimensional Transport Problem

This appendix will outline the steps by which the three-dimensional, time independent, radially symmetric diffusion equation is reduced into a one-dimensional problem. By simplifying the diffusion equation in this manner, the approximating polynomials developed for the one-dimensional problem in chapter III are still applicable.

Beginning with the time independent, spherically symmetric form in three dimensions

$$-D \frac{1}{r^2} \frac{d}{dr} r^2 \frac{dF}{dr} + \Sigma^a F = S \quad (45)$$

Next, a simple substitution is made in equation (45), as follows

$$u(r) = rF(r) \quad (46)$$

By solving equation (46) for  $F$ , substituting back into equation (45) and collecting terms, the resulting equation is

$$-D \frac{1}{r} \frac{d^2 u}{dr^2} + \Sigma^a \frac{u}{r} = S \quad (47)$$



Which simplifies to the form

$$-D \frac{d^2 u}{dr^2} + \Sigma^a u = S' \quad (48)$$

$$\text{where} \quad S' = rS \quad (49)$$

Equation (48) is in a form similar to the one dimensional diffusion equation (chapter III, equation (26)) and can be solved using the same basic code, with the modification to the source term given by equation (49). Hence each group in the multigroup diffusion problem is solved in terms of the variable  $u$ , and the fluence at each node is obtained by applying equation (46).

## Appendix D: The Analytical Solution (Simple Case)

In order to verify the radiation transport code, it is necessary to look at a simple case of the diffusion equation, and obtain a solution analytically. Hence, a simple two energy group problem will be considered, and the diffuse solution for the lower energy group will be solved.

First, the homogeneous solution to equation (48) in appendix C must be found

$$-D \frac{d^2 u}{dr^2} + \Sigma^a u = 0 \quad (50)$$

The homogeneous solution follows quite easily, and by requiring the solution to remain finite with increasing range,  $r$ , it reduces to one term.

$$u_h(r) = C \exp(-(\Sigma^a/D)^{1/2} r) \quad (51)$$

Next, the particular solution to equation (48) is determined by first assigning  $u$  as

$$u_p(r) = A_1 r + A_0 \quad (52)$$

By differentiating equation (52) twice with respect to  $r$  and substituting back into equation (48) from appendix C, the

result becomes

$$\Sigma^a A_1 r + \Sigma^a A_0 = rS \quad (53)$$

By equating the like terms of equation (53), the coefficients are determined as follows

$$A_0 = 0 \quad (54)$$

$$A_1 = S/\Sigma^a \quad (55)$$

The final solution becomes

$$u(r) = C \exp(-(\Sigma^a/D)^{\frac{1}{2}} r) + S/\Sigma^a r \quad (56)$$

To determine the constant C, the first boundary must be applied. Since there is only virgin flux at the origin of the source, the diffuse solution must be zero when r is zero, and hence

$$u(0) = C = 0 \quad (57)$$

Equation (56) now reduces to one term, and when it is solved for the fluence by applying equation (46) (appendix C), it becomes

$$F(r) = S(r)/\Sigma^a \quad (58)$$

The initial intensity levels assigned to these two energy groups were 0.40 counts per photon (group 1) and 0.35 counts per photon (group 2). The values of the diffusion constant and macroscopic absorption cross section were  $2.6637\text{E}+4$  cm,  $5.8079\text{E}-5/\text{cm}$ ,  $2.6232\text{E}+4$  cm and  $5.5647\text{E}-5/\text{cm}$ , in that order. The results for the diffuse solution using the analytical solution was  $4.01\text{E}-11$  counts per photon per square cm, and the transport code solution for only one mesh space was  $8.65\text{E}-12$  counts per photon per square cm.

## Appendix E: Transport Code Listing

This appendix provides a listing of the radiation transport code discussed in chapter III. The subroutines are discussed one at a time, along with a brief description of the variables. Variables which are discussed in the main program will not be discussed a second time in each subroutine.

When running this code, it is very important to make dimensional changes to two of the variables, in order to maintain the positive definite nature of the arrays which are processed by the IMSL library subroutines. These include the S array in the main program and the S and the MG arrays in subroutine diff. The S array must be dimensioned as a NV \* 3 matrix and MG as a NV \* 4 matrix. Here NV stands for the number of variables, and is equal to two times the number of nodes. As listed, the program is set up for 100 mesh spaces, or 202 variables (the flux and current at each node). If the number of mesh spaces is changed without redimensioning these two arrays accordingly, the IMSL subroutines will return error messages.

Another important note concerning this program concerns the lines containing a "D" where a comment code "C" would normally go. These lines are debugging lines, and are compiled on the Harris 800 when the debug mode is used, otherwise they are treated as comment lines (not compiled).

This code is written in Fortran 77, and extensive use

was made of references (1) and (9), as well as Dr. Donn Shankland's knowledge of the operating system. The IMSL documentation was also extremely helpful for solving the matrix equations in this program.

### Program Description

#### Main Program.

The main program is responsible for calling all the subroutines and finally printing out the final solution for the fluence at each node.

#### List of Variables.

R - stores the ranges from the source,  
XTR - stores the transport cross sections,  
XR - stores the removal cross sections,  
XT - stores the total cross sections,  
XS - stores the scattering cross sections,  
SG - stores one group's removal cross sections,  
C - stores the boundary conditions c1,c2,d1,d2,  
B - stores the boundary conditions e1,e2  
DD - stores the diffusion constants for one group,  
S - stores the source matrix from Simpson's approx.,  
C1,C2,D1,D2 - boundary conditions,  
E1,E2 - boundary conditions,  
T - stores values of 1,  $2\pi$  &  $4\pi$ ,  
MAXN - maximum number of nodes,  
MAXMAT - maximum number of materials (1 in this prob.),  
N - number of nodes,

K - geometry factor,  
MAT - stores the material number,  
NMAT - number of materials,  
NC - IMSL subroutine variable,  
I - integer counter,  
NV - number of variables,  
MAXG - number of groups used.

Subroutine GDATA.

This subroutine retrieves the basic data for setting up the appropriate mesh spacing.

List of Variables.

A, AA, B, BB, C - position variables,  
NR - number of regions,  
MN - material number,  
NS - number of mesh spaces per region,  
M - position variable.

Subroutine MDATA.

This subroutine retrieves data on each different group and each different material.

List of Variables.

I, J, K - integer counters.

Subroutine BDATA.

This subroutine retrieves the boundary data and sets up the C matrix.

Subroutine BOUNDR.

This subroutine computes the boundary condition matrix, C, in the case of the radiation transport problem, due to the

energy dependent boundary conditions.

Subroutine DIRECT.

This subroutine calculates the direct fluence at the nodal points and at the midpoints of each mesh interval, values which are modified in subroutine TERM and ultimately used in the Simpson's approximation.

List of Variables.

GROUP - the current group number,  
IA - the current interval number (mesh space),  
GAMMA - stores the initial intensity levels of  
all the groups,  
DPHI - stores the direct fluence at each node,  
MPHI - stores the direct fluence at each  
half node,  
MULT - temporary storage variable,  
MIDPT - the midpoint of the interval.

Subroutine TERM.

This subroutine modifies the direct fluences into the source term used by the Simpson's approximation.

List of Variables.

IH - group counter for downscatter calculations,  
MSOURCE - source term at mid-interval,  
DR - distance from the left node to the  
midpoint of the current interval.

Subroutine DIFF.

This subroutine sets up and solves the matrix equation derived in chapter III. In arriving at the solution for the



```

C
C      solve for lambdas
C
D      PRINT*,''
D      PRINT*,'entering LEQT1P to solve for lamdas'
      CALL LEQT1P (Q,1,2,R,2,ID,D1,D2,IR)
D      PRINT*,' solution follows (lamdas):'
D      PRINT*,' LAMDA 1 =' ,R(1)
D      PRINT*,' LAMDA 2 =' ,R(2)
C
C      add boundary terms to the free solution
C
D      PRINT*,' entering SAXPY to add in boundary terms . . .'
      DO 7 I = 1,2
          CALL SAXPY (NV,R(I),S(1,I+1),1,S,1)
7      CONTINUE
D      PRINT*,''
D      PRINT*,' the solution for the variable U follows'
D      PRINT*,' (for fluence*r AND current*r)'
D      PRINT*,' (still in subroutine DIFF)'
D      DO 500 IP = 1,NV
          PRINT*,S(IP,1),S(IP,2),S(IP,3)
D500 CONTINUE
C      since the solution is in terms of the arbitrary
C      variable "U", which is equal to R * FLUENCE,
C      we must now SOLVE for the scattered fluence by
C      dividing "U" by R at each node and putting the
C      solution back in the matrix "S".
      DO 600 I = 1,NV,2
          IX = I - (I/2 - 0.5)
          XX(1) = 1
D          PRINT*,'S(' ,I,' ,1) =' ,S(I,1)
D          PRINT*,'XX(' ,IX,' ) =' ,XX(IX)
          S(I,1) = S(I,1)/XX(IX)
D          PRINT*,S(I,1)
600 CONTINUE

```

```

C
C      solve the main matrix problem
C
D      PRINT*,''
D      PRINT*,' entering LEQ1PB . . .'
D      PRINT*,''
D      CALL LEQ1PB (MG,NV,3,NV,S,NV,3,IDGT,D1,D2,IER)
D      PRINT*,''
D      PRINT*,' the solution for t0, t1 & t2 follows:'
D      DO 138 IY = 1,NV
D          PRINT*,S(IY,1),S(IY,2),S(IY,3)
D138      CONTINUE
C
C      compute the small matrix
C
D      K=0
D      PRINT*,''
D      PRINT*,'entering VIPRFF imsl subroutine now...'
D      PRINT*,''
D      PRINT*,''
D      PRINT*,'the pre-VIPRFF C matrix follows:'
D      DO 145 IT = 1,NV
D          PRINT*,C(IT,1),C(IT,2)
D145      CONTINUE
D      DO 200 I = 1,2
D          CALL VIPRFF (C(1,I),S,NV,1,1,R(I))
D          PRINT*,''
D          PRINT*,'for i =',I
D          PRINT*,'R(' ,I,') =',R(I)
D          PRINT*,'B(' ,I,') =',B(I)
D          R(I) = B(I) - R(I)
D          PRINT*,'B(I) - R(I) =',R(I)
D          DO 150 J = 1,I
D              K = K + 1
D              PRINT*,''
D              PRINT*,' entering VIPRFF again ...'
D              CALL VIPRFF(C(1,I),S(1,J+1),NV,1,1,Q(K))
D              PRINT*,'      for j=',J
D              PRINT*,'      and k =',K
D              PRINT*,'      Q(' ,K,') =',Q(K)
D150      CONTINUE
D200      CONTINUE

```



```

C
C      now, build each local matrix (for each interval)
C
NI = N-1
D  PRINT*, 'N = ', N
D  PRINT*, 'NV = ', NV
D  PRINT*, 'NI = ', NI
DO 100 IA = 1, NI
    D=DD(IA)
    H=XX(IA+1) - XX(IA)
D  PRINT*, 'for interval number', IA
D  PRINT*, ' D = ', D
D  PRINT*, ' XX(IA+1) = ', XX(IA+1)
D  PRINT*, ' XX(IA) = ', XX(IA)
D  PRINT*, ' H = ', H
D  PRINT*, 'SG(IA) = ', SG(IA)
D  PRINT*, ''
    ML(1,1,IA)=1.2*D/H + 13.*SG(IA)*H/35.
    ML(2,1,IA)=-0.1 - 11.*SG(IA)*H*H/(210.*D)
    ML(3,1,IA)=-1.2*D/H + 9.*SG(IA)*H/70.
    ML(4,1,IA)=-0.1 + 13.*SG(IA)*H*H/(420.*D)
    ML(2,2,IA)=(D/(30.*H)+H*SG(IA)/420.) * (2.*H/D)**2
    ML(3,2,IA)=-ML(4,1,IA)
    ML(4,2,IA)=-(D/(30.*H)+H*SG(IA)/140.) * (H/D)**2
    ML(3,3,IA)=ML(1,1,IA)
    ML(4,3,IA)=-ML(2,1,IA)
    ML(4,4,IA)=ML(2,2,IA)
C      now fill in the rest of the elements
DO 30 I = 1,3
    IP = I + 1
    DO 20 J = IP,4
        ML(I,J,IA) = ML(J,I,IA)
20    CONTINUE
30    CONTINUE
D  PRINT*, ''
D  PRINT*, ' echo the local matrix now . . .'
D  DO 35 IZ = 1,4
D      PRINT*, ML(IZ,1,IA), ML(IZ,2,IA), ML(IZ,3,IA), ML(IZ,4,IA)
035 CONTINUE
C
C      assemble the global matrix now
C
K=IA+IA-2
DO 50 I = 1,4
    DO 40 J = 1,I
        MG(K+I,4+J-I)=MG(K+I,4+J-I)+ML(I,J,IA)
40    CONTINUE
50    CONTINUE
D  PRINT*, ''
D  PRINT*, '-----'
D  PRINT*, '      GROUP', IG, '      INTERVAL', IA
D  PRINT*, '-----'
D  PRINT*, ''

```

```
*****
*                               SUBROUTINE DIFF                               *
*****
```

```
      SUBROUTINE DIFF(S,C,B,XX,DD,SG,NV,N,NG,XS,XT,MAT,IG,T)
```

```
      INTEGER NV,N,NI,IG,IH,INSCATTER,NG,MAT(*),K,IA
      REAL D,DD(*),H,SG(*),SA,SB,SC,SOURCE(101),T(3)
      + ,D1,D2,MG(22,4),ML(4,4,100),S(22,3),C(202,2)
      REAL B(*),R(2),Q(3),XX(101),XS(5,21,21),DPHI(101),XT(5,21)
      + ,MPHI,MIDPT,MSOURC,PHI(18,101)
```

```
      C
      C      This subroutine uses the FINITE ELEMENTS METHOD to
      C      solve the one-dimensional diffusion equation.
```

```
      C
      C      MA = 1/(30*H) *
      C      | 36
      C      | -3H/D   (2H/D)**2
      C      | -36    3H/D      36
      C      | -3H/D   -(H/D)**2  3H/D   (2H/D)**2
      C
      C      MB = H/420 *
      C      | 156
      C      | -22H/D   (2H/D)**2
      C      | 54      -13H/D      156
      C      | 13H/D   -3(H/D)**2  22H/D   (2H/D)**2
```

```
      C
      C      note: these matrices come from the quadratic terms of the
      C      penalty function and are symmetric (hence the blank
      C      entrees in the upper portions).
```

```
      C
      C      NV = 2 * N
      D      PRINT*,'echo of C matrix within subroutine diff...'
      D      PRINT*,''
      D      DO 10 I = 1,NV
      D          PRINT*,C(I,1),C(I,2)
      D10  CONTINUE
      C          ZERO THE ARRAYS
      C          DO 3 I = 1,NV
      C          DO 4 J = 1,3
      C              ZERO OUT THE GLOBAL MATRIX
      C              MG(I,J) = 0.0
      C          ZERO OUT THE SOURCE MATRIX
      C          S(I,J) = 0.0
      C          4 CONTINUE
      C          ZERO OUT THE LAST COLUMN OF THE GLOBAL MATRIX
      C          MG(I,4) = 0.0
      C          3 CONTINUE
```

```
*****
*                               SUBROUTINE TERM                               *
*****
```

```

SUBROUTINE TERM (N,MAT,IG,IH,R,XS,PHI,SOURCE,
+   MPHI,MIDPT,IA,MSOURC,XT)

REAL R(101),XS(5,21,21),PHI(18,101),SOURCE(*),MPHI,MIDPT,
+   MSOURC,DR,XT(5,21)
INTEGER N,MAT(*),IG,IH,IA

C      this subroutine computes the source term which is used
C      in the Simpson's Rule Approximation for the integrand
C      term: -2FSprime.
C      NOTE: since Sprime = rS, the source term becomes:
C              XS * R * DPHI
C
D      PRINT*,''
D      PRINT*, 'in subroutine TERM ..'
D      PRINT*,''
D      PRINT*, 'IG =',IG, 'IH =',IH
      DO 200 I = 1,N-1
          SOURCE(I) = XS(MAT(I),IG,IH)*PHI(IH,I)*R(I)
200    CONTINUE
      SOURCE(N) = XS(MAT(N-1),IG,IH)*PHI(IH,N)*R(N)
D      PRINT*, '(IG STILL ',IG,')      IH =',IH
D      PRINT*, 'XS(IG,IH) =',XS(MAT(N-1),IG,IH)
C      now calculate the 4(pi)r**2 fluence at the left side of
C      this interval . . .
      MIDPT = 0.5 * (R(IA) + R(IA+1))
      MPHI = 4 * 3.1415926 * (R(IA)**2) * PHI(IH,IA)
      DR = MIDPT - R(IA)
D      PRINT*, 'R(IA) =',R(IA), ' MIDPT =',MIDPT, ' DR =',DR
D      PRINT*, ' IA =',IA, ' & IA+1 =',IA+1
C      calculate the fluence at mid-interval using
C      exponential loss by absorption ONLY (sigma removal).
      MPHI = MPHI * EXP(-XT(MAT(IA),IH)*DR) / (4*3.141593*MIDPT**2)
      MSOURC = XS(MAT(IA),IG,IH) * MPHI * MIDPT
D      PRINT*, ' MSOURC =',MSOURC
D      PRINT*, ' SOURCE(IA) =',SOURCE(IA)
D      PRINT*, ' SOURCE(IA+1) =',SOURCE(IA+1)
      END

```

```

C
C      assign the geometry factor "K" in next line.
C
      K = 2
      MULT = GAMMA(GROUP)
C      iterate over all the nodes
      DO 100 I = 1,N
        IF (I.EQ.1) THEN
          R(I) = 1
C        i.e., set the left boundary = 1 cm
          DPHI(1) = MULT/(T(K)*R(1)**K)
          ELSE
            H(I) = R(I) - R(I-1)
            MULT = MULT*EXP(-XT(MAT(I-1),GROUP)*H(I))
            DPHI(I) = MULT/(T(K)*R(I)**K)
          ENDIF
100    CONTINUE
C      ends loop over all nodes
C
C      now calculate the third direct fluence value, that is,
C      the value in the middle of the interval of interest.
C
      MIDPT = 0.5 * (R(IA) + R(IA+1))
      MPHI = GAMMA(GROUP) * EXP(-XT(MAT(IA),GROUP)*MIDPT)
      +      / (T(K) * MIDPT**K)
D      PRINT*, 'DPHI at IA =', IA, ' is =', DPHI(IA)
D      PRINT*, 'DPHI at IA+1 =', IA+1, ' is =', DPHI(IA+1)
D      PRINT*, 'MPHI =', MPHI
D      PRINT*, 'MIDPOINT =', MIDPT
      END

```

```

*****
*                               SUBROUTINE DIRECT                               *
*****

```

```

      SUBROUTINE DIRECT (N,T,R,MAT,XT,DPHI,GROUP,IA,MPhi,MIDPT)
C
C      this subroutine computes the direct fluence at each
C      node for each group, filling the "DPHI" array.
C
      REAL R(*),XT(5,21),DPHI(101),GAMMA(18),T(3),MULT,H(101)
      + ,MPhi,MIDPT
      INTEGER N,K,MAT(*),GROUP,IA
D      PRINT*,' '
D      PRINT*,' in subroutine DIRECT . . .'
D      PRINT*,' '
D      PRINT*,'GROUP =',GROUP
      GAMMA(1) = 0.0
      GAMMA(2) = 0.0
      GAMMA(3) = 0.0
      GAMMA(4) = 0.0
      GAMMA(5) = 0
      GAMMA(6) = 0.33
      GAMMA(7) = 0.13
      GAMMA(8) = 0.05
      GAMMA(9) = 0.10
      GAMMA(10) = 0.25
      GAMMA(11) = 0.01
      GAMMA(12) = 0.03
      GAMMA(13) = 0.03
      GAMMA(14) = 0.04
      GAMMA(15) = 0
      GAMMA(16) = 0.03
      GAMMA(17) = 0
      GAMMA(18) = 0

```



```

*****
*                               SUBROUTINE BOUNDOR                               *
*****
      SUBROUTINE BOUNDOR(C,C1,C2,D1,D2,DD,SG,N,NV)
      REAL C(202,2),C1,C2,D1,D2,DD(*),SG(*)
      INTEGER N, NV

C
C      This subroutine sets up the C-matrix for each energy
C      group & passes it back to the main program. This
C      subroutine is necessary in the radiation transport
C      problem ONLY when the boundary conditions require terms
C      that are energy dependent.
C
      D2 = (DD(N-1)*SG(N-1))*0.5
D      PRINT*,''
D      PRINT*,N-1 =',N-1,'DD =',DD,'SG =',SG
      C(1,1) = C1
      C(2,1) = D1
      C(NV-1,2) = C2
      C(NV,2) = D2
D      PRINT*,'echo of C-matrix in subroutine BOUNDOR:'
D      DO 100 I = 1,NV
D          PRINT*,C(I,1),C(I,2)
D100  CONTINUE
      END

```

```

*****
*                               SUBROUTINE BDATA                               *
*****

      SUBROUTINE BDATA (MAXG,NG,NV,C1,C2,D1,D2,E1,E2,C)
C
C      this subroutine reads in boundary data and
C      computes the boundary matrix.
C
      REAL E1(*),E2(*),C1,C2,D1,D2,C(202,2)
      INTEGER MAXG,NG,I,NV
D      PRINT*,' entering BDATA subroutine . . . '
      PRINT*,'ENTER C1,C2,D1,D2 (AS SHOWN)'
      READ*,C1,C2,D1,D2
      PRINT*,'ENTER ONE VALUE OF E1 FOR EACH ENERGY GROUP'
      PRINT*,'BEGIN WITH HIGHEST GROUP (#1), PUTTING EACH ENTRY'
      PRINT*,'ON A SEPARATE LINE.'
      DO 80 I = 1,NG
          READ*,E1(I)
      80  CONTINUE
      PRINT*,'NOW REPEAT FOR E2'
      DO 90 I = 1,NG
          READ*,E2(I)
      90  CONTINUE
C
C      now construct the "C" matrix (boundary cond. matrix)
C
      C(1,1) = C1
      C(2,1) = D1
      C(NV-1,2) = C2
      C(NV,2) = D2
D      PRINT*,'echo the C matrix in BDATA subroutine'
      DO 100 I = 1,NV
          PRINT*,C(I,1),C(I,2)
      100 CONTINUE
      END

```

```

*****
*                               SUBROUTINE MDATA                               *
*****

```

```

      SUBROUTINE MDATA(MAXMAT,MAXG,NMAT,NG,XTR,XT,XS,XR)
C
C      this subroutine reads in material data.
C
      REAL XTR(5,21),XT(5,21),XS(5,21,21),XR(5,21)
      INTEGER NG,MAXMAT,MAXG,NMAT,I,J,K
D      PRINT*,''
D      PRINT*,' entering MDATA subroutine now . . .'
D      PRINT*,''
      PRINT*,'ENTER THE NUMBER OF DIFFERENT MATERIALS USED'
      READ*,NMAT
      PRINT*,'ENTER THE TOTAL NUMBER OF ENERGY GROUPS'
      READ*,NG
C      read in cross sections beginning with transport and total
      DO 20 I = 1,NMAT
        DO 60 J = 1,NG
          PRINT*,'ENTER MATERIAL',I,', GROUP',J,' CROSS SECTIONS'
          PRINT*,'sigma tr, sigma t: SEPARATE BY COMMAS.'
          READ*,XTR(I,J),XT(I,J)
C      now read in the scatter cross sections
          PRINT*,'NOW ENTER THE SCATTERING CROSS SECTIONS.'
          PRINT*,'BEGIN WITH SCATTER FROM HIGHEST ENERGY GROUP'
          PRINT*,'AND STEP THROUGH GROUPS UNTIL WITHIN GROUP SCATTER'
          PRINT*,'EX. 1->IG, 2->IG, ....., (IG-1)->IG, IG->IG'
          DO 70 K = 1,J
            READ*,XS(I,J,K)
          70      CONTINUE
C      compute the removal cross section from total and scatter
          XR(I,J) = XT(I,J) - XS(I,J,J)
        60      CONTINUE
      20      CONTINUE
      MAXG = NG
      END

```

```
*****
*                               SUBROUTINE GDATA                               *
*****
```

```

SUBROUTINE GDATA (MAXN,MAXMAT,R,MAT,N,K)
REAL R(*)
REAL A,B,C
INTEGER NR,K,AA,MN,NS,BB,M,MAT(*),N,I

PRINT*, 'ENTER THE NUMBER OF REGIONS'
READ*,NR
PRINT*, 'ENTER THE LEFT BOUNDARY LOCATION'
READ*,A
PRINT*, 'ENTER THE GEOMETRY TYPE, K=?'
READ*,K
AA=1
DO 50 I = 1,NR
  PRINT*, 'ENTER THE RIGHT HAND BOUNDARY FOR REGION ',I
  READ*,B
  PRINT*, 'ENTER THE # OF MESH SPACES FOR THIS REGION'
  READ*,NS
  PRINT*, 'ENTER THE MATERIAL NUMBER'
  READ*,MN
  C = (B-A)/NS
  BB = AA + NS
  DO 5 M = AA,BB
    IF (M.EQ.AA) THEN
      R(M)=A
    ELSE
      R(M) = A + C
      A = R(M)
    ENDIF
  CONTINUE
  DO 10 M = AA, BB-1
    MAT(M) = MN
  CONTINUE
  AA = BB
  N = BB
  MAXN=N
  MAXMAT = BB-1
50 CONTINUE
END
```

```

*****
*                               MULTI-GROUP DIFFUSION EQUATION CODE          *
*                               (WITH FINITE ELEMENT METHOD)                  *
*                               *                                           *
*                               DATE WRITTEN:  28 OCT 1984                    *
*                               *                                           *
*                               AUTHOR:      L. WAYNE BRASURE                *
*                               *                                           *
*****

```

```

REAL R(101),XTR(5,21),XR(5,21),XT(5,21),XS(5,21,21),SG(100)
REAL C(202,2),B(2),DD(100),S(22,3)
REAL C1,C2,D1,D2,E1(21),E2(21),T(3)
INTEGER MAXN,MAXMAT,N,K,MAT(100),NMAT,NC,I,NV,NG,MAXG
T(0) = 1
T(1) = 6.2832
T(2) = 12.5664
MAXG = 21
D PRINT*, 'entering data entry phase of program ...'
D PRINT*, ''
CALL GDATA (MAXN,MAXMAT,R,MAT,N,K)
NV = N * 2
CALL MDATA(MAXMAT,MAXG,NMAT,NG,XTR,XT,XS,XR)
CALL BDATA(MAXG,NG,NV,C1,C2,D1,D2,E1,E2,C)
D PRINT*, ''
D PRINT*, 'echo of C matrix within main program . . .'
D PRINT*, ''
D DO 10 I = 1, NV
D PRINT*, C(I,1),C(I,2)
D10 CONTINUE
DO 999 IG=1,NG
DO 50 I = 1, N-1
SG(I) = XR(MAT(I),IG)
DD(I) = 1./(3.*XTR(MAT(I),IG))
D PRINT*, 'echo SG(' ,I, ') = ',SG(I)
D PRINT*, 'echo DD(' ,I, ') = ',DD(I)
50 CONTINUE
B(1) = E1(IG)
B(2) = E2(IG)
CALL BOUND(C,C1,C2,D1,D2,DD,SG,N,NV)
CALL DIFF(S,C,B,R,DD,SG,NV,N,NG,XS,XR,MAT,IG,T)
PRINT*, ''
PRINT*, ''
PRINT*, ' THE SOLUTION FOLLOWS === GROUP',IG
PRINT*, ''
PRINT*, ''
D PRINT*, S(NV-1,1)
DO 60 I = 1,NV,2
IX = I - (I/2 - 0.5)
PRINT*, ' at R =',R(IX), 'cm, F =',S(I,1)
60 CONTINUE
C now end the iteration over all energy groups . . .
999 CONTINUE
END

```

fluxes and currents at each node, it sets up the local and global matrices for each group (one at a time), performs the Simpson's approximation, and solves the series of matrix equations (using IMSL subroutines) in order to arrive at the solution for each group. Each group calculation is performed separately, beginning with the highest energy group, group one. The solution is stored in the S matrix, printed out, and then the subroutine moves on to the next lower group.

List of Variables.

NI - the number of mesh intervals,  
INSCATTER - 1 if doing an inscatter calculation,  
D - diffusion constant in current interval,  
H - width of current interval,  
SA, SB, SC - variables used in Simpson's approx.,  
SOURCE - stores the source term used in Simpson's  
approx.,  
XX - stores the positions of each node,  
R, Q - variables used in solving linear equations  
in conjunction with IMSL subroutines.

```

C
C      we now have the FLUENCE due to scattering and
C      must add this to the direct fluence at each node.
C
C      first, we must calculate the direct fluence for this
C      energy group at each node.
C
      CALL DIRECT(N,T,XX,MAT,XT,DPHI,IG,IA,MPhi,MIDPT)
      PRINT*, '-----'
      PRINT*, ''
      PRINT*, ' Scattered Fluence for Group',IG,' is ',S(NV-1,1)
      PRINT*, ' & the Direct Fluence =',DPHI(N)
      DO 700 I = 1,NV,2
        IX = I -(I/2 - 0.5)
        PRINT*, 'S(',I,',',1) =',S(I,1)
        PRINT*, 'DPHI(',IX,',') =',DPHI(IX)
        S(I,1) = S(I,1) + DPHI(IX)
        PRINT*, 'S(',I,',',1) =',S(I,1)
        C      put the solutions for this energy group into the
        C      "PHI" array, to be used for the downscattered
        C      contribution for the lower energy groups.
        PHI(IG,IX) = S(I,1)
        PRINT*, ' for IX =',IX,' and IG =',IG
        PRINT*, ' PHI(IG,IX) =',PHI(IG,IX), ' S(I,1) =',S(I,1)
      700 CONTINUE
      C
      C      return control
      C
      END

```

## Appendix F: Generating Poisson and Multinomial Reference Values

This appendix briefly discusses the way in which the reference source spectra were arrived at for both the Poisson and multinomial versions of the Bayes' theorem analysis. Both methods use the numbers generated by the "channel percentage converting program" which is listed in this appendix. This program converts the raw transport data contained in tables III-1 through III-6 into a form acceptable to the Bayes' theorem analysis codes discussed in appendix H.

### Program Algorithm and Use

For each of the three sources at each of the ranges given, the program inputs the number of counts per photon in each channel. The program output includes the total counts per photon for the given source as well as a listing of the proportion of counts in each channel (the sum of all channels being unity).

The total counts per photon value is used to determine the total number of counts for each source at any given distance. For instance, if at a distance of 50 meters, measurements of equal time (Poisson) or of equal counts (multinomial) yield 10,000 counts (assigned arbitrarily), then the number of counts at all other ranges can be determined for all sources. For source A at 100 meters, the



total counts per photon (all channels) of source A is divided by the total counts per photon (all channels) of source A at 50 meters, and multiplied by the number of counts at 50 meters. This yields the following:  $9.12\text{E}-10/3.16\text{E}-9 * 10000 = 2816.7$ . So that 2816.7 counts will be obtained (2817 for the multinomial analysis). The reference sources will be constructed from this type of data, as discussed in the next two sections.

#### Poisson Reference Sources

The first step in the process is to assign a level of counts at the 50 meter range. Then, using the method discussed above, the number of counts for all three sources at each range is calculated. Next, using the proportion of counts in each channel, the number of counts in each channel is determined. This results in three reference sources at each range.

#### Multinomial Reference Sources

To obtain the multinomial reference sources, the total number of counts for each source at each range is determined in the same manner as above. The reference sources at each range consist simply of the proportions in each channel (recall the form of the multinomial distribution).

#### Program Output

The output from this program has been suppressed, since

it follows readily from tables III-1 through III-6.

List of Variables

integer:

COUNTS = counts/photon in each channel,

N = source number (1-3),

NN = scientific notation subroutine variable,

SUM = total counts/photon (all channels),

real:

XX = scientific notation subroutine variable.

```

10 REM
20 REM ++++++
30 REM +
35 REM +   CHANNEL % CONVERTING PROGRAM   +
40 REM +       By L. Wayne Brasure       +
50 REM +       December 1984             +
55 REM +                                   +
60 REM ++++++
70 REM
80 DIM COUNTS(18)
85 INPUT " Enter the source number =>";N
90 INPUT " Enter the range (in meters) =>";RANGE
100 PRINT " Enter the counts per photon for each channel indicated : "
110 SUM = 0
120 FOR I = 1 TO 18
130 PRINT " Channel Number ";I;" =>"
140 INPUT COUNTS(I)
150 SUM = SUM + COUNTS(I)
160 NEXT I
170 PRINT "For Source Number ";N;" , at R = ";RANGE;" meters:"
175 PRINT
180 PRINT "      total counts per photon =";SUM
185 PRINT
190 PRINT "      (channel breakdown follows)"
200 PRINT
210 PRINT "      CHANNEL NUMBER           PERCENT OF TOTAL COUNTS"
220 PRINT "      _____"
225 PRINT ""
230 NN = 4
235 REM      ++++++      print out the table now . . .
240 FOR I = 1 TO 18
250 COUNTS(I) = COUNTS(I) / SUM
253 PRINT "      ";
255 XX = I: GOSUB 2100: PRINT "      ";
260 XX = COUNTS(I)
270 GOSUB 2100
275 PRINT
280 NEXT I
290 PRINT
300 INPUT " Care for another run? Enter [1] for yes =>";ANS
310 IF (ANS = 1) GOTO 85
320 END

```

```

2100 REM
2110 REM      ++++++
2120 REM      +   SCIENTIFIC NOTATION SUBROUTINE   +
2190 REM      ++++++
2200 REM
2210 REM
2220 IF NN < 0 OR NN > 8 THEN PRINT "RANGE ERR";: RETURN
2230 EX = 0: IF XX = 0 THEN MT$ = "0.": GOTO 2250
2240 MT = VAL ( STR$ ( ABS (XX))): GOSUB 2260: IF NN < 8 THEN MT = MT + .
      5 * 10 ^ ( - NN): GOSUB 2260
2250 PRINT MID$ ("+-",(XX < 0) + 1,1); LEFT$ (MT$ + "00000000",NN + 2);"
      E"; MID$ ("+-",(EX < 0) + 1,1); RIGHT$ ("0" + STR$ ( ABS (EX)),2): RETURN
2260 IF MT > = 10 THEN MT = MT / 10:EX = EX + 1: GOTO 2260
2270 IF MT < 1 THEN MT = MT * 10:EX = EX - 1: GOTO 2270
2280 MT$ = STR$ (MT): IF MID$ (MT$,2,1) < > "." THEN MT$ = MT$ + "."
2290 RETURN

```

## Appendix G: Generating Measured Source Spectra

This appendix will address the method of generating the measured source spectra during the analysis section of the problem. The method will be discussed separately for each of the three types of statistical distributions used.

### Poisson Random Number Generator ref. (11) & (16)

#### Algorithm Description.

The Poisson distribution inputs the reference sources in the form of number of counts in each channel (units = counts), unlike the multinomial distribution format. One of the three reference sources is selected as the source which is to be "measured," and the measured source array is initially assigned as this particular reference source.

The Poisson random number subroutine first generates a random number between between 0 and 1 (inclusive) and assigns the value to the variable NUM. An integer is incremented, beginning at 1, and is stored in the variable N. The probability of obtaining this number N is calculated using the Poisson distribution with the number of reference counts in the channel serving as the mean. The probability is next compared with the random number, and the integer N is increased until the probability is greater than the random number, NUM. This process is repeated for all 18 channels.

#### List of Variables.

integer:

IG = channel counter,  
N = number of measured counts,  
U = number of counts,  
real:  
MPHI(18) = measured source array (ends up an integer),  
NUM = random number variable,  
P = probability variable,  
T = probability variable,  
Y = number of reference counts variable.

Gaussian Random Number Generator ref. (16)

Algorithm Description.

The Gaussian random number generator begins in the same manner as does the Poisson random number generator, with the MPHI array initially equal to the chosen reference source. Next, for each channel of the measured source, twelve random numbers are generated, since the uniform random number generator approximates the Gaussian distribution with this many repetitions (16). Each time a random number is generated, it is added to the number of counts in the given channel less 6. After all the numbers have been generated, the resultant real number of counts is rounded to an integer number of counts.

List of Variables.

integer:  
IG = channel counter,  
IMPHI(18) = final measured source array,

real:

MPHI(18) = initial measured source array,

X = random number variable,

Y = reference counts in a channel minus 6.

#### Multinomial Random Number Generator ref. (16)

##### Algorithm Description.

Unlike the Poisson and Gaussian distributions, the multinomial distribution subroutine inputs the reference sources as fractions of counts in each channel (units = counts/photon). To generate a measured spectrum, one of the reference sources is selected as before. The fractions in each channel are converted into a cumulative distribution, so that the last channel in the MPHI array will contain a value of 1.

The multinomial random number generator then assigns each one of the total counts available to one of the channels in the measured source array as follows. First, a random number between 0 and 1 is generated, which is then compared with the cumulative probability in each channel of the MPHI array. When the random number is less than the cumulative probability in one of the channels, the count is added to that particular channel. This process continues until all the available counts have been depleted, leaving a new measured source spectrum.

##### List of Variables.

integer:

I = total count incrementor,  
IG = channel number counter,  
MPHI(18) = measure source array,  
NC(18) = counting array,  
SUM = total number of counts available,  
T = channel number counter,  
real:  
X = random number variable.

#### Subroutine Listings.

The random number generators are listed with the main analysis programs in appendix H.



## Appendix H: Analysis Code Listings

This appendix describes and lists the three codes used to generate the measured source spectra and perform the Bayes' theorem analysis. There is one code for each of the statistical distributions used: Poisson, Gaussian and multinomial. The first code listed is the Poisson version, and will be listed in its entirety. To obtain the Gaussian code, two subroutines need to be replaced: the RANDOM subroutine and the POISSON subroutine. Subroutine RANDOM was discussed in appendix F, and will not be discussed further. The listing of the two new subroutines (RANDOM and GAUSSIAN) begins on page 132. Similarly, in the multinomial code, only those subroutines which are different from the Poisson code will be listed and described. The multinomial listing begins on page 133.

All analysis codes were written in BASIC to run on the Apple II series of computers, and minor modifications will translate them into forms which can be run on almost any microcomputer.

### The Bayes' with Poisson Program

#### Main Program.

The main program inputs the number of channels (energy groups) and the range at which the analysis will be performed. It then calls the subroutines to solve for the Bayes' posterior distribution, and prints out the results.

The calculations are performed for one measured source at a time at one range.

List of Variables.

RPHI - stores the three reference source spectra,  
MPHI - stores the measured source spectrum,  
NC - stores the number of counts in each channel  
of the measured spectrum,  
P - stores  $P(X|A_i)$  value of each source,  
H\$ - string array used in reading data  
from data files,  
RANGE - distance from the source at which the  
analysis is performed,  
NG - the number of channels in each source,  
P1, P2, P3 - comprise the posterior distribution,  
NN, XX - scientific notation variables,  
ANS - integer value 1 continues program  
execution.

Subroutine REFERENCE.

This subroutine retrieves the reference sources from data files stored on disk. It feeds the data into the RPHI array.

Subroutine MEASURED.

This subroutine fills up the MPHI array with the values from whichever source has been selected.

Subroutine RANDOM.

This subroutine generates the measured source spectrum using the Poisson distribution. Refer to appendix F for

details on this subroutine.

#### Subroutine BAYES.

This subroutine performs the Bayes' theorem analysis as depicted in equation (30) of chapter IV.

#### List of Variables.

A1, A2, A3 - the assumed prior distribution  
of the reference sources,  
DENOM - stores the denominator in equation (30),  
X1, X2, X3 - the values of  $P(X|A_i)$  returned by  
subroutine POISSON.

#### Subroutine POISSON.

This subroutine calculates the values of  $P(X|A_i)$  using the Poisson distribution, as discussed in chapter IV.

#### List of Variables.

S - reference source counter,  
P - stores the final values of  $P(X|A_i)$ ,  
IG - channel counter,  
I - count level counter,  
FT - temporary storage variable,  
TERM - temporary storage variable.

#### Scientific Notation Subroutine.

This "canned" subroutine formats the output on the Apple IIe computer and was written by John Baldwin of Erie, Pennsylvania.

#### Data Retrieval Subroutine.

This subroutine retrieves text data from disk and converts it into numerical data for use in the program.

### The Bayes' with Gaussian Program

Listing begins on page 132.

#### Main Program.

The main program is identical to the Poisson version, and hence, only the two new subroutines will be discussed.

#### Subroutine RANDOM.

This subroutine generates the measured source spectrum using the Gaussian distribution. Refer to appendix F for details on this subroutine.

#### Subroutine GAUSSIAN.

This subroutine calculates the values of  $P(X|A_i)$  using the Gaussian distribution, as discussed in chapter IV.

### The Bayes' with Multinomial Program

Listing begins on page 133.

#### Main Program.

The main program is basically the same as the Bayes' with Poisson program, so once again, only the new subroutines will be discussed.

#### Subroutine MEASURED.

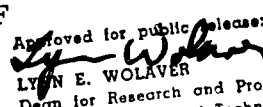
The modification to this subroutine is to calculate the cumulative probability in each channel of the array MPHI, in order to calculate a measured spectrum using the multinomial random number generator discussed in appendix F.

#### Subroutine RANDOM.

This subroutine generates the measured source spectrum

This report shows that gamma ray spectra identification using Bayes' Probability Theorem can be used to extend positive identification ranges when compared with the method of photopeak identification. In this study, Bayes' Theorem methodology extended the range of positive identification a minimum of 50 meters in a low count environment. These results are based on spectra generated using the Finite Element Method in conjunction with Poisson counting statistics.

# REPORT DOCUMENTATION PAGE

1a. REPORT SECURITY CLASSIFICATION <b>UNCLASSIFIED</b>			1b. RESTRICTIVE MARKINGS		
2a. SECURITY CLASSIFICATION AUTHORITY			3. DISTRIBUTION/AVAILABILITY OF REPORT  Approved for public release; distribution unlimited.		
2b. DECLASSIFICATION/DOWNGRADING SCHEDULE					
4. PERFORMING ORGANIZATION REPORT NUMBER(S)  AFIT/GNE /PH/85M-2			5. MONITORING ORGANIZATION REPORT NUMBER(S)		
6a. NAME OF PERFORMING ORGANIZATION  School of Engineering		6b. OFFICE SYMBOL (If applicable)  AFIT/EN	7a. NAME OF MONITORING ORGANIZATION		
6c. ADDRESS (City, State and ZIP Code)  Air Force Institute of Technology Wright-Patterson AFB, OH 45433			7b. ADDRESS (City, State and ZIP Code)		
8a. NAME OF FUNDING/SPONSORING ORGANIZATION		8b. OFFICE SYMBOL (If applicable)	9. PROCUREMENT INSTRUMENT IDENTIFICATION NUMBER		
8c. ADDRESS (City, State and ZIP Code)			10. SOURCE OF FUNDING NOS.		
			PROGRAM ELEMENT NO.	PROJECT NO.	TASK NO.
11. TITLE (Include Security Classification)  See Box 19			WORK UNIT NO.		
12. PERSONAL AUTHOR(S)  L. Wayne Brasure, B.S., M.S.S.M., CAPT, USAF					
13a. TYPE OF REPORT  M.S. Thesis		13b. TIME COVERED FROM _____ TO _____	14. DATE OF REPORT (Yr., Mo., Day)  1985, March		15. PAGE COUNT
16. SUPPLEMENTARY NOTATION					
17. COSATI CODES			18. SUBJECT TERMS (Continue on reverse if necessary and identify by block number)		
FIELD	GROUP	SUB. GR.	Gamma Ray Spectra, Bayes' Theorem, Remote Detection, Radioactive Materials.		
20	08				
19. ABSTRACT (Continue on reverse if necessary and identify by block number)					
<p>Title: Identification of Nuclear Materials from Remote Detection of Characteristic Gamma Rays</p> <p>Thesis Chairman: Leslie L. McKee, MAJOR, USAF</p> <p style="text-align: right;">Approved for public release: 1AW AFR 190-1    LYNN E. WOLAVER  Dean for Research and Professional Development  Air Force Institute of Technology (AFIT)  Wright-Patterson AFB OH 45433</p>					
20. DISTRIBUTION/AVAILABILITY OF ABSTRACT  UNCLASSIFIED/UNLIMITED <input checked="" type="checkbox"/> SAME AS RPT. <input type="checkbox"/> DTIC USERS <input type="checkbox"/>			21. ABSTRACT SECURITY CLASSIFICATION  UNCLASSIFIED		
22a. NAME OF RESPONSIBLE INDIVIDUAL  Leslie L. McKee, MAJOR, USAF			22b. TELEPHONE NUMBER (Include Area Code)  (513) 255-4498		22c. OFFICE SYMBOL  AFIT/ENP

## VITA

Captain L. Wayne Brasure was born to the Reverend and Mrs. Lloyd G. Brasure on February 21, 1958 in Petoskey, Michigan. He grew up in Northville, Michigan and graduated from Northville High School in June of 1976. He received his B.S. degrees in Physics and Astronomy from the University of Michigan, Ann Arbor, Michigan in December of 1980, and was commissioned through AFROTC on the same date. His first assignment was with the Western Space and Missile Center, Air Force Systems Command, at Vandenberg AFB, CA, where he worked as an Advanced Space Systems Requirements Manager (WSMC/XR). He received the Master of Science Degree in Systems Management from the University of Southern California in June of 1983 and was assigned to the Air Force Institute of Technology in August of the same year.

Permanent address: 20990 Taft Road  
Northville, MI 48167

14. McLaren, Capt Robert D. A Code for Aircraft Survivability Analysis - Gamma and Neutron Effects. MS Thesis. School of Engineering, Air Force Institute of Technology (AU), Wright-Patterson AFB OH, June 1972.
15. Shankland, Donn G., PhD. Lecture notes presented in NE 7.05, Radiation Transport. School of Engineering, Air Force Institute of Technology (AU), Wright-Patterson AFB OH, July - September 1984.
16. Shankland, Donn G., PhD. Personal conversation. Department of Engineering Physics, School of Engineering, Air Force Institute of Technology (AU), Wright-Patterson AFB OH, July - December 1984.
17. Winkler, Robert L. An Introduction to Bayesian Inference and Decision. New York: Holt, Rinehart and Winston, Inc., 1972.



### Bibliography

1. Ageloff, Roy and Richard Mojena. Applied Fortran 77. Belmont, CA: Wadsworth Publishing Company, Inc., 1981.
2. Anderson, T. W. An Introduction to Multivariate Statistical Analysis. New York: John Wiley & Sons, Inc., 1958.
3. Becker, Eric B. et. al. Finite Elements, An Introduction, Volume 1. Englewood Cliffs, New Jersey: Prentice-Hall, Inc., 1981.
4. Bevington, Philip R. Data Reduction and Error Analysis for the Physical Sciences. New York: McGraw-Hill Book Company, Inc., 1969.
5. Clark, Melville and Kent F. Hanson. Numerical Methods of Reactor Analysis. New York: Academic Press, Inc., 1964.
6. Desai, C. S. Elementary Finite Element Method. Englewood Cliffs, New Jersey: Prentice-Hall, Inc., 1979.
7. Dooley, Lt Alan W. Study of Total Gamma Spectra Correlation for Extending Identification Range Over Photopeak Analysis. MS Thesis, AFIT/GNE/PH/84M-2. School of Engineering, Air Force Institute of Technology (AU), Wright-Patterson AFB OH, January 1984.
8. Duderstadt, James J. and William R. Martin. Transport Theory. New York: John Wiley & Sons, 1979.
9. Etter, D. M. Structured Fortran 77 for Scientists and Engineers. Menlo Park, California: The Benjamin/Cummings Publishing Company, Inc., 1983.
10. Graybill, Franklin A. and Alexander M. Mood. Introduction to the Theory of Statistics. New York: McGraw-Hill Book Company, Inc., 1963.
11. Handscomb, D. C. and J. M. Hammersley. Monte Carlo Methods. London: Methuen & Co. LTD, 1964.
12. Hardin, David D. Numerical Methods of Radiation Transport. Class notes. School of Engineering, Air Force Institute of Technology (AU), Wright-Patterson AFB, OH, July 1980.
13. Kshirsagar, Anant M. Multivariate Analysis. New York: Marcel Dedder, Inc., 1972.

```

5550 REM  +++++ Now factor in the last few factorial terms:
5560 TI = SUM - TI - 1
5565 IF (TI < 1) GOTO 5600
5570 FOR I = TI TO 1 STEP - 1
5580 P(S) = P(S) * I
5590 NEXT I
5600 NEXT S
5610 X1 = P(1): PRINT "X1 = ";X1
5620 X2 = P(2): PRINT "X2 = ";X2
5630 X3 = P(3): PRINT "X3 = ";X3
5700 RETURN
5800 REM  +++++ a factorial fix-all begins here:
5810 P(S) = P(S) * (SUM - TI)
5820 TI = TI + 1
5830 GOTO 5240

```

```

5000 REM
5010 REM ++++++
5020 REM +      SUBROUTINE MULTINOMIAL      +
5030 REM ++++++
5040 REM
5050 REM +++++ Bubble sort the MPHI array, and place
5060 REM +++++ the RPHI values in a corresponding order.
5062 SWITCH = 1
5063 IF (SWITCH = 0) GOTO 5080: REM (go to end statement).
5064 SWITCH = 0: REM (0 if sort is complete)
5065 FOR I = 2 TO NG
5066 IF (MPHI(I) < MPMH(I - 1)) GOTO 5068
5067 GOTO 5078
5068 TEMP = MPMH(I)
5069 MPMH(I) = MPMH(I - 1)
5070 MPMH(I - 1) = TEMP
5071 REM +++++ Now, the fractions must move WITH the MPMH sort:
5072 FOR IV = 1 TO 3
5073 T9 = RPHI(IV,I)
5074 RPHI(IV,I) = RPHI(IV,I - 1)
5075 RPHI(IV,I - 1) = T9
5076 NEXT IV
5077 SWITCH = 1
5078 NEXT I
5079 GOTO 5063
5080 REM +++++ Bubble sort is now complete . . .
5090 REM +++++ Now, calculate the P(X|source 1), etc.
5100 FOR S = 1 TO 3
5150 P(S) = 1
5200 IM = MPMH(NG)
5210 JL = 1: TI = 1
5220 P(S) = SUM
5230 FOR I = 1 TO IM
5240 IF (TI < SUM AND P(S) < 1E30) GOTO 5800
5250 IF ((MPMH(JL) - I) < 0) GOTO 5300
5260 GOTO 5500
5300 JL = JL + 1
5400 GOTO 5250
5500 FOR J = JL TO NG
5510 P(S) = P(S) * RPHI(S,J) / I
5520 NEXT J
5530 NEXT I

```

```

2000 REM
2010 REM ++++++
2015 REM +      SUBROUTINE MEASURED      +
2020 REM ++++++
2025 REM
2030 PRINT : PRINT "MEASURED SOURCE SPECTRUM": PRINT "-----
-----"
2040 PRINT "      at ";RANGE;" cms.": PRINT
2050 PRINT "enter the applicable ref. source (1,2,or3) :": PRINT
2055 PRINT " (the cumulative prob. will be calculated)"
2057 INPUT I
2060 FOR IG = 1 TO NG
2065 FRAC(TIG) = PHI(I,IG)
2081 MPHI(IG) = FRAC(TIG)
2085 IF (IG > 1) THEN MPHI(IG) = MPHI(IG) + MPHI(IG - 1)
2090 PRINT " MPHI(";IG;") = ";MPHI(IG);" FRAC(TIG) = ";FRAC(TIG)
2100 NEXT IG
2110 RETURN
3000 REM
3010 REM ++++++
3020 REM +      SUBROUTINE RANDOM      +
3030 REM ++++++
3040 REM
3041 REM +++++ initialize the counter array:
3042 FOR T = 1 TO 18:NC(T) = 0: NEXT T
3060 FOR I = 1 TO SUM
3065 X = RND (1)
3070 FOR IG = 1 TO NG
3080 Y = X - MPHI(IG)
3090 IF (Y < 0) THEN GOTO 3100
3095 NEXT IG
3100 NC(IG) = NC(IG) + 1
3110 NEXT I
3120 PRINT : PRINT " Measured source spectrum follows:": PRINT
3125 FOR IB = 1 TO 3: PRINT CHR$(7): NEXT IB
3130 FOR IG = 1 TO NG
3140 PRINT " channel # ";IG;" = ";NC(IG)
3150 MPHI(IG) = NC(IG)
3155 NEXT IG
3200 RETURN

```

```

3000 REM
3010 REM ++++++
3020 REM + SUBROUTINE RANDOM +
3030 REM ++++++
3040 REM
3050 REM +++++ This subroutine generates random numbers
3060 REM +++++ FOLLOWING A GAUSSIAN DISTRIBUTION . . .
3070 FOR IG = 1 TO NG
3080 Y = MPHI(IG) - 6.0
3090 FOR J = 1 TO 12
3100 X = RND (1)
3200 Y = Y + X
3210 NEXT J
3220 MPHI(IG) = Y
3230 IF (MPHI(IG) < 0) THEN MPHI(IG) = 0
3240 NEXT IG
3300 REM +++++ Echo the measured source spectrum:"
3310 PRINT CHR$ (7); PRINT CHR$ (7)
3320 PRINT "Measured source spectrum follows:"; PRINT
3330 FOR IG = 1 TO NG
3335 IMPHI(IG) = INT (MPHI(IG) + 0.5)
3340 PRINT "channel ";IG;" = ";IMPHI(IG)
3350 NEXT IG
3360 PRINT
3400 RETURN

5000 REM
5010 REM ++++++
5020 REM + SUBROUTINE GAUSSIAN +
5030 REM ++++++
5040 REM
5100 FOR S = 1 TO 3
5110 P(S) = 1
5120 DUMMY = 1
5130 FOR IG = 1 TO NG
5140 IF (IMPHI(IG) > 0) GOTO 5200
5150 ZT = 1
5160 GOTO 5300
5200 ZT = IMPHI(IG)
5300 DUMMY = EXP ( - 0.5 * ((IMPHI(IG) - RPHI(S,IG)) / ZT ^ 0.5) ^ 2) / (
2 * 3.142593 * ZT) ^ 0.5
5310 P(S) = P(S) * DUMMY
5320 NEXT IG
5330 NEXT S
5440 X1 = P(1); PRINT "X1 = ";X1
5450 X2 = P(2); PRINT "X2 = ";X2
5460 X3 = P(3); PRINT "X3 = ";X3
5500 RETURN

```

```

5000 REM
5010 REM ++++++
5020 REM + SUBROUTINE POISSON +
5030 REM ++++++
5040 REM
5050 FOR S = 1 TO 3
5060 P(S) = 1
5070 FT = 1
5080 DUMMY = 1
5090 FOR IG = 1 TO NG
5100 REM +++++ calculate factorial in numerator
5110 FT = 1
5120 FOR I = 1 TO MPHI(IG)
5130 FT = FT * I
5140 NEXT I
5160 IF (RPHI(S,IG) > 0) GOTO 5300
5170 TERM = 1
5180 GOTO 5400
5300 TERM = RPHI(S,IG) ^ MPHI(IG)
5400 DUMMY = EXP ( - RPHI(S,IG)) * TERM / FT
5410 P(S) = P(S) * DUMMY
5420 NEXT IG
5430 NEXT S
5440 X1 = P(1): PRINT "X1 = ";X1
5450 X2 = P(2): PRINT "X2 = ";X2
5460 X3 = P(3): PRINT "X3 = ";X3
5500 RETURN
6000 REM
6010 REM ++++++
6020 REM + SCIENTIFIC NOTATION SUBROUTINE +
6090 REM ++++++
6100 REM
6110 REM
6120 IF NN < 0 OR NN > 8 THEN PRINT "RANGE ERR";: RETURN
6130 EX = 0: IF XX = 0 THEN MT$ = "0.": GOTO 6150
6140 MT = VAL ( STR$ ( ABS (XX))): GOSUB 6160: IF NN < 8 THEN MT = MT + .
5 * 10 ^ ( - NN): GOSUB 6160
6150 PRINT MID$ ("+-",(XX < 0) + 1,1); LEFT$ (MT$ + "00000000",NN + 2);"
E"; MID$ ("+-",(EX < 0) + 1,1); RIGHT$ ("0" + STR$ ( ABS (EX)),2);: RETURN
6160 IF MT > = 10 THEN MT = MT / 10:EX = EX + 1: GOTO 6160
6170 IF MT < 1 THEN MT = MT * 10:EX = EX - 1: GOTO 6170
6180 MT$ = STR$ (MT): IF MID$ (MT$,2,1) < > "." THEN MT$ = MT$ + "."
6190 RETURN
7000 REM
7010 REM ++++++
7020 REM + DATA RETRIEVAL SUBROUTINE +
7030 REM ++++++
7040 GET C$
7050 IF C$ = R$ THEN RETURN
7060 H$(IG) = H$(IG) + C$
7070 GOTO 7040

```

```

3000 REM
3010 REM ++++++
3020 REM +          SUBROUTINE RANDOM          +
3030 REM ++++++
3040 REM
3050 REM +++++ This subroutine generates random numbers
3060 REM +++++ following a Poisson distribution . . .
3070 FOR IG = 1 TO NG
3080 Y = MPHI(IG)
3100 IF (Y <= 0) GOTO 3300
3110 NUM = RND (1)
3120 N = 0
3130 T = EXP ( - Y)
3140 P = T
3150 REM +++++ The DO UNTIL loop begins here:
3160 IF (NUM <= P) GOTO 3400
3170 N = N + 1
3190 U = N
3200 T = T * Y / U
3210 P = P + T
3220 GOTO 3160
3300 REM +++++ else, N = 0:
3310 N = 0
3400 REM +++++ assign new value of MPHI(IG)
3410 MPHI(IG) = N
3500 NEXT IG
3510 PRINT CHR$(7): PRINT CHR$(7)
3600 PRINT : PRINT " the measured spectrum follows:" : PRINT
3610 FOR IG = 1 TO NG
3620 PRINT " channel ";IG;" = ";MPHI(IG)
3630 NEXT IG
3700 RETURN
4000 REM
4010 REM ++++++
4020 REM +          SUBROUTINE BAYES          +
4030 REM ++++++
4040 REM
4050 REM +++++ First, assign the prior oistribution values
4060 REM +++++ of the three reference sources . . .
4070 A1 = 0.3333:A2 = 0.3333:A3 = 0.3333
4080 REM +++++ Call the statistics subroutine to
4090 REM +++++ determine the values of P(X|source 1),
4100 REM +++++ P (X|source 2), and P (X|source 3).
4110 GOSUB 5000
4120 REM +++++ Calculate the denominator term of Bayes' Thm.
4130 DENOM = X1 * A1 + X2 * A2 + X3 * A3
4135 IF (DENOM = 0) THEN PRINT " DENOM = 0:" : GOTO 4200
4140 REM +++++ calculate the likelihoods at the reference
4150 REM +++++ range from the source.
4155 FOR IB = 1 TO 3: PRINT CHR$(7): NEXT IB
4160 P1 = (X1 * A1) / DENOM
4165 P2 = (X2 * A2) / DENOM
4170 P3 = (X3 * A3) / DENOM
4200 RETURN

```

```

1000 REM ++++++
1010 REM +          SUBROUTINE REFERENCE          +
1020 REM ++++++
1030 REM
1040 PRINT : PRINT "REFERENCE SOURCES": PRINT "-----"
1050 PRINT "      at a range of ";RANGE;" cms"
1055 PRINT
1056 PRINT " now acquiring necessary data . . ."
1057 D$ = CHR$ (4): REM +++++ (ESCAPE CHARACTER)
1058 R$ = CHR$ (13): REM +++++ (RETURN CHARACTER)
1059 PRINT D$;"OPEN SOURCE DATA"
1060 PRINT D$;"READ SOURCE DATA"
1070 FOR I = 1 TO 3
1080 REM +++++ loop through all three sources
1090 FOR IG = 1 TO NG
1100 REM +++++ loop through all the channels
1110 GOSUB 7000
1120 RPHI(I,IG) = VAL (H$(IG))
1130 H$(IG) = ""
1140 NEXT IG
1150 NEXT I
1155 PRINT R$
1160 PRINT D$;"CLOSE SOURCE DATA"
1170 PRINT "ECHO DATA . . ."
1180 PRINT : FOR I = 1 TO 3
1185 PRINT " SOURCE # ";I
1190 FOR IG = 1 TO NG
1200 PRINT " channel ";IG;" = ";RPHI(I,IG)
1210 NEXT IG
1220 NEXT I
1500 RETURN
2000 REM
2010 REM ++++++
2015 REM +          SUBROUTINE MEASURED          +
2020 REM ++++++
2025 REM
2030 PRINT : PRINT "MEASURED SOURCE SPECTRUM": PRINT "-----"
      PRINT "-----"
2040 PRINT "      at ";RANGE;" cms.": PRINT
2050 PRINT "enter the applicable ref. source (1,2,or3) ": PRINT
2055 PRINT " (the cumulative prob. will be calculated)"
2057 INPUT I
2060 FOR IG = 1 TO NG
2065 FRAC(I,IG) = RPHI(I,IG)
2081 MPHI(IG) = FRAC(I,IG)
2090 PRINT " MPHI(";IG;" ) = ";MPHI(IG)
2100 NEXT IG
2110 RETURN

```



```

10 REM
20 REM ++++++
30 REM +
40 REM + BAYES PROBABILITY ANALYSIS +
50 REM + (using the Poisson distribution) +
60 REM + By: L. Wayne Brasure +
70 REM + December 1984 +
80 REM +
90 REM ++++++
100 REM
110 DIM RPHI(3,18): DIM MPHI(18): DIM NC(18): DIM FRACT(18)
111 DIM P(3): DIM H$(18)
115 PRINT "random number seed = "; RND ( - 7)
118 PRINT : PRINT : HOME
120 PRINT "BAYES PROBABILITY ANALYSIS"
130 PRINT "(the multinomial version w/no background . . .)"
140 PRINT : PRINT
150 INPUT "Enter the total number of channels => "; NG
160 INPUT "Enter the distance from the source (cms) => "; RANGE
170 REM +++++ enter the reference source spectra at this range
180 GOSUB 1000
190 REM +++++ enter the measured source spectrum @ this range
200 GOSUB 2000
210 REM +++++ Calculate measured source spectrum
215 REM +++++ using POISSON random number generator
220 GOSUB 3000
230 REM +++++ Calculate the Bayesian Posterior Distribution
240 GOSUB 4000
245 IF (DENOM = 0) GOTO 360
250 REM +++++ Print out the Posterior Distribution
260 NN = 4
265 PRINT
270 PRINT " SOURCE NUMBER          PROB (SOURCE(i) $\frac{1}{2}$ X)"
280 PRINT " _____          _____"
290 PRINT
300 PRINT "      A                      ";
310 XX = P1: GOSUB 6000: PRINT
320 PRINT "      B                      ";
330 XX = P2: GOSUB 6000: PRINT
340 PRINT "      C                      ";
350 XX = P3: GOSUB 6000: PRINT
360 PRINT : INPUT " Another run perhaps?  $\frac{1}{2}$  1=yes  $\frac{1}{2}$  => "; ANS
370 IF (ANS < > 1) GOTO 995
371 INPUT " . . . with the same setup?"; ANS
372 IF (ANS = 1) GOTO 500
380 INPUT " . . . with just a new MEASURED source? => "; ANS
390 IF (ANS = 1) GOTO 190
400 PRINT " okay, from the beginning then . . ."
410 GOTO 140
500 FOR IG = 1 TO NG
505 MPHI(IG) = FRACT(IG)
520 NEXT IG
530 GOTO 210
995 PRINT : PRINT "Very well then, good day sir."
999 END

```

using the multinomial distribution. Refer to appendix F for details on this subroutine.

Subroutine MULTINOMIAL.

This subroutine calculates the values of  $P(X|A_i)$  using the multinomial distribution, as discussed in chapter IV.

List of Variables.

SWITCH - on/off determining variable for the  
bubble sort,

T9 - a temporary storage variable for the  
bubble sorting process,

JL, TI - incremental markers for the  
multinomial calculations,

SUM -number of the total fixed number of counts  
available.

**END**

**FILMED**

**11-85**

**DTIC**